Food Hydrocolloids 171 (2026) 111862

Contents lists available at ScienceDirect

Food Hydrocolloids

journal homepage: www.elsevier.com/locate/foodhyd

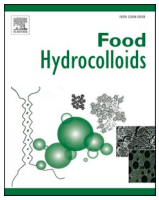

Characterisation of alginate extracted from *Saccharina latissima* with deep eutectic solvents

Wimar Reynaga-Navarro [a], Lucas Bozzo [b], René H. Wijffels [a,c], Michel Eppink [a], Antoinette Kazbar [a,*]

[a] Bioprocess Engineering, Wageningen University, PO Box 16, Wageningen, 6700 AA, the Netherlands
[b] Food Quality and Design Group, Wageningen University, PO Box 17, Wageningen, 6700 AA, the Netherlands
[c] Faculty of Biosciences and Aquaculture, Nord University, Bodø, N-8049, Norway

ARTICLE INFO

Keywords:
Alginate
Deep eutectic solvents
brown seaweed
Extraction
Rheology

ABSTRACT

This study evaluates the impact of using deep eutectic solvents (DES), specifically betaine-urea, as a novel extraction technology for alginate from brown seaweed and its effect on the techno-functionality of the final product. Ten eutectic mixtures were assessed, with betaine-urea (BU) demonstrating the highest performance, yielding 14.9 ± 2.0 % of the total amount of alginate in the first extraction step (BU-1). Although this yield was lower than the conventional acid-alkaline (AK) method (37.6 ± 4.1 %), a sequential extraction combining water (BU-2) and alkaline conditions (BU-3) achieved higher overall yields for the BU method. The study highlights significant differences in the chemical and rheological properties of alginates extracted with BU compared to those obtained via traditional methods. BU-extracted alginates exhibited the characteristic shear-thinning behaviour of alginate solutions but with markedly higher apparent viscosity at low shear rates. BU-2 displayed gel-like behaviour (*tan* δ = 0.1) with a consistency index (*K*) 62 times higher than the acid-alkaline extract. Chemical analysis revealed a higher fraction of high-molecular-weight alginates in BU-2 and BU-3, partially explaining their increased viscosity. However, the role of betaine-urea in shaping the alginate structure and function should be further studied. This research underscores the potential of DES technology in enhancing the functionality of alginate, offering a potentially more sustainable alternative to mineral acid-base methods.

1. Introduction

Alginate, a natural hydrocolloid primarily extracted from brown seaweed, is widely valued for its mechanical and rheological properties, as well as its biocompatibility. It is widely used as a thickening and gelling agent in the food industry and has found applications in the medical field for drug delivery and wound dressings (Abasalizadeh et al., 2020; Yong & Mooney, 2012; Zhang et al., 2023). Moreover, alginate has gained increasing attention in the biotechnology sector as a scaffold material for the growth of animal cells (Hurtado et al., 2022; Sahoo & Biswal, 2021).

Chemically, alginate is an anionic polysaccharide composed of β-D-mannuronic acid (M) and α-L-guluronic acid (G) pyranose units, linked via (1 → 4) glycosidic bonds. These units are arranged in distinct blocks along the linear chain, consisting of homopolymeric regions of poly-M or poly-G, as well as heteropolymeric blocks of alternating MG sequences (Draget, 2009; Rinaudo, 2007). The functionality of alginate is closely related to its chemical structure. Key parameters such as the M/G ratio, the distribution of MM, GG, and MG blocks, and the molecular weight profile play a decisive role in its performance (Draget, 2009; Gomez et al., 2009; Jørgensen et al., 2007, pp. 2388–2397; Rinaudo, 2007). These factors directly influence alginate thickening capacity and its gelling behaviour in the presence of divalent cations such as Ca^{2+}, for instance. Therefore, characterising rheological properties, such as viscosity, viscoelastic behaviour, and gelling strength, is essential to fully evaluate the performance of extracted alginate. Furthermore, linking these functional properties to alginate's chemical composition is crucial, especially given the growing demand for materials with improved or tailored properties to meet new market needs (Rahman et al., 2024).

The characterisation of extracted alginate is key to evaluating its applicability. The molecular weight and the M/G ratio are typically measured as indicators of viscosity and gelling capacity, respectively.

* Corresponding author.
E-mail address: antoinette.kazbar@wur.nl (A. Kazbar).

https://doi.org/10.1016/j.foodhyd.2025.111862
Received 21 May 2025; Received in revised form 14 July 2025; Accepted 11 August 2025
Available online 11 August 2025

For example, measuring the alginate molar mass is a complex task and involves the determination of parameters such as weight average molecular weight (*Mw*) and number average molecular weight (*Mn*) (Agilent Technologies Inc, 2015; Shrivastava, 2018). *Mw* is heavily influenced by the presence of high molecular weight units, while *Mn* is the average of all units of alginate present in the sample. Both parameters are used to calculate the polydispersity index (PDI), an important parameter in polymers which describes the distribution of all sizes present in a sample of alginate (Gomez et al., 2009). Similarly, measuring the M/G is a critical parameter to be carefully determined via a controlled hydrolysis process, so the analysis reflects as closely as possible the original structure of the alginate (Bojorges, López-Rubio, Fabra, et al., 2023). These parameters can then be linked with the rheological properties of the alginate in solution and after forming a gel, offering insights into its potential applications.

The behaviour of the alginate in dispersion can be evaluated through viscosity measurements at different shear rates, as well as by determining its storage and loss modulus (G' and G'') under oscillation. Following gelation, typically induced by divalent cations, the physical properties of the resulting gels can be characterised using a texture profile analysis. (Farrés & Norton, 2014; Hermansson et al., 2016; J. Yang et al., 2009). Understanding these properties is key to establishing a clear link between the extraction process and its final functional performance.

Alginate extraction is often limited by the robustness of the seaweed cell wall, a complex matrix composed of sulphated fucans, polyphenols, proteins, cellulose, and alginate itself (Deniaud-Bouët et al., 2014; Shao & Duan, 2022). This structure is difficult to disassemble, making extraction challenging. The conventional extraction process involves multiple steps using harsh chemicals (Fig. 1).

After harvesting, seaweed is either processed fresh, preserved by drying, or pretreated with formalin. While formalin enhances storage stability and improves extraction efficiency and alginate quality (Saji et al., 2022), its toxicity and environmental impact are major concerns. The extraction begins with the acidification step using dilute sulfuric or hydrochloric acid to remove divalent cations and form insoluble alginic acid. This is followed by alkaline extraction with sodium carbonate, resulting in soluble sodium alginate. The solution, initially highly viscous, is diluted for easier handling. Debris is removed by flotation and filtration, and the permeate is bleached and acidified to precipitate alginate fibres (Bojorges, López-Rubio, Martínez-Abad et al., 2023; Saji et al., 2022). These fibres are subsequently washed, neutralised, and dried to yield sodium alginate, which is finally characterised. Alternative processes using ethanol or calcium precipitation are also employed, depending on the desired product (Saji et al., 2022).

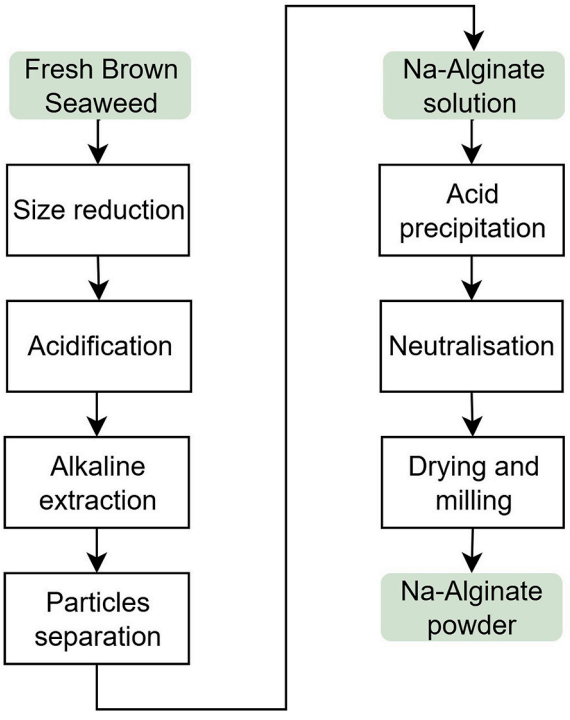

Fig. 1. Flowchart of alginate via acid-alkaline extraction process based on Saji et al., 2022.

The aforementioned conventional technology used for alginate extraction involves multiple chemical-intensive steps and can significantly affect the structural properties of alginate, especially molecular weight and blocks of M-G distribution (Bojorges, López-Rubio, Martínez-Abad et al., 2023; Gomez et al., 2009). Thus, new technologies for milder extraction and processing of seaweed biomass for alginate recovery have been intensively explored (Bojorges, López-Rubio, Martínez-Abad et al., 2023; Lomartire & Gonçalves, 2022).

In recent years, Deep Eutectic Solvents (DES) have emerged as promising alternatives to conventional extraction solvents. DES are defined as mixtures of a hydrogen bond acceptor (HBA) and a hydrogen bond donor (HBD) whose strong interaction reduces the melting point compared to the individual components (Abbott et al., 2003; Naik et al., 2022). A widely studied example is choline chloride–urea (reline), which forms a liquid at room temperature when mixed in a 1:2 M ratio, despite the high melting points of the individual components. Another notable group of DES employs betaine (trimethylglycine) as the hydrogen bond acceptor (HBA) and has also been the subject of several studies (Abranches et al., 2020, 2021; Alcalde et al., 2024; Aroso et al., 2017).

DES offer remarkable versatility, as they can be designed from biodegradable and non-toxic compounds such as sugars, polyols, amino acids, and organic acids, resulting in what are known as Natural Deep Eutectic Solvents (NaDES) (Liu et al., 2018). Their tunable composition allows adjustment of solvent properties to target specific molecules, whether polar or non-polar.

Given these properties, DES have been explored for the extraction of bioactive compounds from biomass. For example, pigments such as fucoxanthin and bacterioruberin have been successfully extracted using menthol-based DES (Kholany et al., 2023, 2025). However, the extraction of macromolecules like polysaccharides remains more challenging. Research has demonstrated the potential of DES for extracting carrageenan (Das et al., 2016), chitin (Saravana, Ho, et al., 2018; Wang et al., 2022), and brown seaweed polysaccharides such as fucoidan and alginate (Saravana, Cho, et al., 2018), though sometimes at very high water contents (>70 %) where the DES structure may be disrupted (El Achkar et al., 2019).

More recently, Elizondo et al. (2024) dug into the use of membranes for alginate separation using choline chloride ethylene glycol DES, while Reynaga-Navarro et al. (2024) explored chemical methods to isolate alginate from choline chloride-based DES, suggesting potential interaction of alginate with the tested DES. In this context, Hiemstra et al. (2024) demonstrated that yields up to 70 % can be achieved with choline chloride-urea DES. Although basic chemical characterisation confirmed the presence of functional groups and molecular weight similarities to conventionally extracted alginate, the functionality, particularly the rheological properties, was not evaluated.

In addition to extraction, DES have shown potential as a pretreatment agent and not only as an extraction medium. They have been successfully applied to wood pretreatment to improve pulping processes, for biomass delignification to enhance hemicellulose recovery, and for microalgae cell wall disruption (Li et al., 2023; Loow et al., 2017; Matchim Kamdem et al., 2023; Xu et al., 2020). DES have also been proposed as catalytic platforms and shown to increase cell membrane permeability (Huang et al., 2014; T. X. Yang et al., 2017). Despite DES capabilities as pretreatment agents, research on seaweed is still limited (de Souza Mesquita, 2024).

This study investigated alginate extraction using hydrophilic Deep Eutectic Solvents (DES) through a three-step sequential approach: (1) extraction with DES alone, (2) water extraction of the residual biomass, and (3) alkaline extraction of the final residue. The influence of this DES-based process on the techno-functional properties of the obtained alginates was evaluated by chemical and rheological characterisation and compared to conventionally extracted alginate.

2. Materials and methods

2.1. Biological material

Brown seaweed *Saccharina latissima* (SL) was collected from Kamperland in May 2023 (Zeeland, The Netherlands). The biomass was frozen, stored at −80 °C and used as needed. When needed, the biomass was freeze-dried in a Sublimator 2 × 3 × 3–5 (Zirbus Technology, Germany) for 46 h. Later, the dry seaweed was ground into powder with a particle size in the range of 90 and 710 μm and kept at 4 °C for later use.

2.2. Analytics

2.2.1. Alginate and sugars in dry samples

This procedure was based on the protocol reported by Bojorges et al. (2023). In a 10 mL glass tube, 2 mg of sample were placed and 1 mL of 2 M HCl in anhydrous methanol (Supelco®) was added to perform a methanolysis process. The tube was incubated at 100 °C for 4 h. Later, the tube was cooled down, and the methanol solution was evaporated with a gentle stream of N_2 until apparent dryness. Over the dry pellet, 1 mL of 2 M trifluoracetic acid was added and incubated at 120 °C for 40 min. The tube was then cooled down and dried again with N_2 until apparent dryness. The final dried sample was redissolved in 1 mL of Milli-Q water, filtered (0.22 μm PVDF syringe filter from Millipore) and placed in a plastic vial. As a positive control of methanolysis, 2 mg of standard sodium alginate (88 % purity, Sigma-Aldrich) were subjected to the same process. 10 μL of each sample was injected into a Dionex ICS-6000 HPIC System (Thermo Fisher Scientific™) at 30 °C in a flow rate of 0.5 mL min^{-1} through a Dionex Carbopac™ PA20 (3 × 150 mm) column from ThermoFisher Scientific™ using 100 mM NaOH (A), 500 mM NaOH (B), 500 mM sodium acetate + 50 mM NaOH (C) and Milli-Q water (D) as eluents in conditions as described in Table 1:

Uronic acids and sugars were detected via an electrochemical detector, and concentrations [μg mL^{-1}] were determined using standard curves prepared with D-mannuronic acid (≥90 %, Sigma-Aldrich), L-guluronic acid (≥95 %, BOC Sciences), mannitol (≥99 %, Supelco®), fucose (≥99 %, Supelco®), rhamnose monohydrate (≥99 %, Sigma-Aldrich), arabinose (≥99 %, Sigma-Aldrich), galactose (≥99 %, Sigma-Aldrich), glucose monohydrate (≥99 %, Thermo Scientific), xylose (≥99 %, Sigma-Aldrich) and mannose (≥99 %, Sigma-Aldrich).

The fraction of alginate X_{Alg} was calculated based on the concentration of both uronic acids using Equation (1).

$$X_{Alg} = \frac{W_{UA} * F_{pol}}{F_{Ly} * W_S} \quad \text{Equation 1}$$

Table 1
Gradient conditions for the analysis of uronic acids using the Dionex™.

Time [min]	A [%]	B [%]	C [%]	D [%]
0	4	0	0	96
8	10	0	0	90
13	10	0	0	90
13	8	15	30	52
22	8	15	30	52
22	60	0	0	40
26	4	0	0	96
36	4	0	0	96

Where W_{UA} is the amount of uronic acids detected in the sample [μg]; F_{pol} is the correction factor due to the addition of a water molecule to the monomer during the lysis process, which is defined as $\frac{MW_{mono}}{MW_{UA}}$, where MW_{mono} is the molecular weight [g mol^{-1}] of a monomer unit attached to the polymer and MW_{UA} is the molecular weight [g mol^{-1}] of a uronic acid monomer isolated from the polymer. F_{Ly} is the correction factor based on the lysis efficiency of the standard sodium alginate. F_{Ly} is calculated based on the proportion of uronic acids obtained after the methanolysis process over the uronic acids present in the standard sodium alginate added as a positive control. Finally, W_S is the weight [μg] dry basis of the sample. The fraction of alginate in the sample, denoted as X_{Alg}, when multiplied by 100, represents the alginate purity expressed as a percentage [%].

The M-G ratio was calculated by dividing the concentration of mannuronic acid [μg mL^{-1}] by the concentration of guluronic acid [μg mL^{-1}] in the sample.

2.2.2. Alginate in solutions via colourimetric assay for uronic acids

Alginate in solutions was quantified using a colourimetric assay for uronic acids using the carbazole reaction (Cesaretti et al., 2003). 50 μL of sample solution was placed in a heat-resistant 96-well plate, and 200 μL of 25 mM solution of sodium tetraborate in 97 % sulfuric acid was added and mixed with the sample. The plate was then placed in an oven for 10 min and later cooled down for 15 min. When cooled, 50 μL of 0.125 % carbazole in absolute ethanol was added to the mixture, and the plate was placed in the oven at 100 °C for 10 min. Finally, the plate was cooled down for 15 min, and the mixture was read in a spectrophotometer at 550 nm, and the concentration was determined with a standard curve made with D-galacturonic acid monohydrate (≥97 %). All reagents used were acquired from Sigma-Aldrich.

2.3. DES screening for extraction

2.3.1. DES extractions

Table 2 displays the set of choline chloride-based and betaine-based deep eutectic solvents prepared for the screening phase. This set of DES was prepared by mixing compounds at their corresponding molar ratio. The mixtures were placed in a water bath at 80 °C long enough until the components were visually mixed and no crystals or solids were present. Mixtures were stored at room temperature in airtight conditions until use.

Extractions were performed in glass tubes (n = 2) using freeze-dried seaweed with a SLR of 12.5 mg g^{-1}. An amount of 67 mg of dried biomass was rehydrated at room temperature for 1 h with 0.83 g of Milli-

Table 2
Choline chloride and Betaine-based Deep Eutectic Solvents.

HBA[a]	HBD[a]	Molar ratio [n:n]	Water [%w/w]	Abbreviation
Choline chloride	Urea	1:2	10	CCU
	Ethylene glycol	1:2	10	CCEG
	Propylene glycol	1:2	10	CCPG
	Glycerol	1:2	10	CCGly
	Levulinic acid	1:2	10	CCLev
Betaine	Urea	1:2	10	BU
	Ethylene glycol	1:2	10	BEG
	Propylene glycol	1:2	10	BPG
	Glycerol	1:2	10	BGly
	Levulinic acid	1:2	10	BLev

[a] Choline chloride (≥98 %), betaine (≥98 %), urea (≥99.5 %), ethylene glycol (≥99 %), propylene glycol (≥99.5 %), glycerol (≥99 %) and levulinic acid (≥98 %) obtained from Sigma-Aldrich.

Q. Later, 4.17 g of DES was added. The addition of 0.83 g of water reflects the natural moisture content of fresh seaweed, which was measured at 93 %. The total amount of water in the final mixture (DES + hydration water) was 25 % w/w. The content of the tubes was mixed and placed in a water bath at 55 °C for 1h; samples were vortexed regularly. Finished the extraction time, the tubes were cooled down and centrifuged at 4255 g for 10 min in a Beckman Allegra-X-30R device (from now on, all centrifuge processes to be mentioned were carried out a these conditions unless otherwise stated). The supernatant was collected for alginate recovery and quantification.

The remaining pellet was used for a second extraction. All the pellets were completed with Milli-Q water to 5 mL, and samples were incubated at 55 °C for 1 h. Then tubes were centrifuged, and the supernatant was collected for alginate recovery and quantification.

2.3.2. Acid-alkaline extraction as a control

Freeze-dried seaweed (67 mg) was mixed with 5 mL of 0.2 M H_2SO_4 (pH $\leq$ 1.9). The mixture was agitated in an orbital shaker at 25 °C for 1 h. Later, 3.25 % w/w of Na_2CO_3 is added to the mixture to reach a pH of 10 and incubated in a water bath at 55 °C for 1 h. The mixture was then cooled down to room temperature and centrifuged. The pellet was removed, and the supernatant was collected for alginate recovery and quantification. All this procedure was performed at least by duplicates.

2.3.3. Alginate recovery via ethanolic precipitation

Alginate recovery was determined after ethanol precipitation following the method described by Reynaga-Navarro et al. (2024) with modifications. Any volume of alginate solution was collected and mixed with 4 times a mixture of ethanol-water 80 % v/v + 1 % NaCl w/v to precipitate the alginate (from now on EtOH+1). The mixture was then centrifuged again, the supernatant discarded, and the pellet washed with 2 times the ethanol-water 80 % v/v (from now on EtOH). The sample was then centrifuged once more, the new supernatant discarded, and finally, the pellet was put in contact with a stream of N_2 until apparent dryness. The pellet was stored in dry and cool conditions or dissolved in a known volume of Milli-Q water for alginate analysis.

2.3.4. Extraction yield calculation (EY)

To determine the extraction yield EY [%] Equation (2) was used.

$$EY = \frac{C_{UA} * \frac{V_d}{V_p} * V_s * 0.907}{W_{SW} * X_{Alg.SW}} * 100 \qquad \text{Equation 2}$$

Where C_{UA} is the concentration [mg mL^{-1}] of uronic acids obtained from the colourimetric assay; V_d is the volume of water [mL] in which the pelleted alginate was redissolved; V_p was the volume [mL] subjected to precipitation; V_s is the total volume of solvent [mL] used for the extraction; W_{SW} is the weight [mg] of seaweed; $X_{Alg.SW}$ is the mass fraction of alginate in the used seaweed and 0.907 is the correction factor used to adjust the amount of uronic acids into alginate.

2.4. Extraction and characterisation

2.4.1. BU-alginate extraction

To obtain sufficient alginate extracts for further characterisation, the process was scaled up to a batch of 200 g (n = 3) (Fig. 2). An amount of 2.7 g of freeze-dried seaweed was soaked in a capped-glass bottle with 33.2 g of ultrapure water for 1 h at room temperature. Later, 167 g of Betaine-Urea DES (1:2 + 10 % H_2O) were added, and the extraction process was performed in a shaking water bath at 55 °C for 1 h at 140 rpm. After the extraction, the bottle was cooled down, and the content was placed in 50 mL tubes and centrifuged for 10 min. The supernatant (SN-1) was collected and placed in dialysis tubing SnakeSkin™ (ThermoFisher Scientific) with a 3.5 kDa molecular weight cutoff following a dialysis process of 3 steps at room temperature: 2h, 16 h and 2 h. The dialysis water was replaced after each step. Later, the dialysed supernatant (dSN-1) was collected, the volume measured, and the alginate content determined. The alginate was precipitated with 4 vol of EtOH+1, washed with EtOH, dried under a N_2 flow and ground aided with liquid nitrogen, resulting in powder (BU-1). The residual pellet (P-1) was subjected to further processing. Firstly, the volume occupied by the pellet was completed to 200 mL with ultrapure water, and a second extraction of alginate was performed at 55 °C for 1h at 140 rpm. The mixture was cooled down, placed in 50 mL tubes and centrifuged. The supernatant was collected (SN-2) and dialysed (as done with SN-1) and precipitated with ethanol, washed, dried with N_2 and ground, resulting in powder BU-2. A new residual pellet was formed (P-2). This pellet was further processed. The volume occupied by P-2 was completed with 200 mL of water and sodium carbonate, enough to reach 0.1 M as the final concentration. The mixture was subjected to an extraction process at 55 °C for 1 h at 140 rpm. The new mixture was cooled down, placed in 50 mL tubes and centrifuged. The new supernatant (SN-3) was collected and dialysed (as done with SN-1), resulting in a new liquid (dSN-3) from which alginate was precipitated with alcohol, dried and ground, resulting in powder BU-3. The volume of each supernatant was recorded, and the alginate concentration was measured using colourimetric analysis.

2.4.2. Acid-alkaline alginate extraction

Sodium alginate via the acid-alkaline method was prepared as a control (n = 3) at the same scale. 2.7 g of seaweed were mixed with 200 mL of 0.2 M sulfuric acid in a Schott bottle with constant agitation for 1 h at room temperature. Later, the pH is adjusted to >10 with sodium

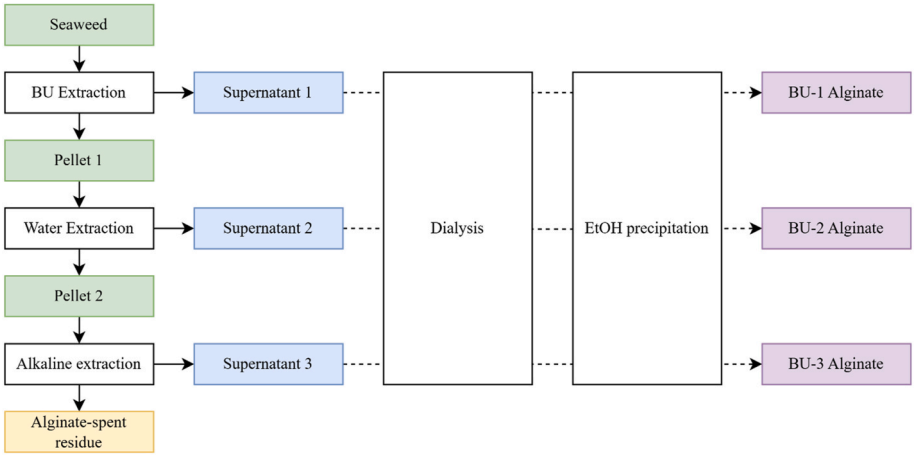

Fig. 2. Flowchart for obtaining BU-Alginate powders.

carbonate, and the mixture is placed in a water bath for extraction at 55 °C for 1h. Following, the mixture is cooled down and placed in 50 mL tubes, centrifuged, and the supernatant collected (SN-AK) and the alginate content determined. This supernatant was subjected to a dialysis process as described for obtaining the BU-Alginates (see section 2.4.2). The dialysed fraction (dSN-AK) was then collected and precipitated with ethanol, dried and milled, obtaining the AK powder.

2.5. Molecular weight (Mw)

Solutions of 0,15 % w/v alginate were prepared in Milli-Q water. 20 μL of sample were injected into an HPLC device 1290 Infinity (Agilent Technologies™) coupled with 2 columns PL aquagel-OH MIXED-H 8um 300 × 7.5 mm (Agilent Technologies™) placed in series. 0.1 M ammonium phosphate monobasic (Sigma-Aldrich) with a pH of 4.5, running at 0.8 mL min^{-1}, was used as eluent. The detection of alginate was performed via a refractive index detector (RID). A standard curve was built with a kit of pullulan standards (PSS-PULKITR1) from Agilent Technologies™. Molecular weights of pullulan were transformed to molecular weights of alginate using the Mark-Houwink relation (Equation (3)).

$$[\eta] = K \cdot M_w^a \quad \text{Equation 3}$$

where $[\eta]$ is intrinsic viscosity in dL g^{-1}, K [dL g^{-1}] and a [−] are the Mark-Houwink parameters, and M_w is the molecular weight of the polymer. The parameters K and a used to calculate $[\eta]$ for the different Mw of the pullulan standards were 1.956 × 10^{-4} dL g^{-1} and 0.667, respectively (Kasaai, 2006); while the ones used for alginate were 1.4 × 10^{-4} dL g^{-1} and 0.92 (Holme et al., 2008). Using this new standard curve, the predicted Mw was calculated with the retention time (RT) observed in the chromatogram. Each chromatogram was split into fractions of 0.1 min, and areas (proportional to intensity c_i) of each fraction were determined with the software of the HPLC device. Each fraction of area also corresponded to a value of molecular weight M_i. Later, the average molecular weight (M_w) and the average molecular number (M_n) were determined with Equation (4) and Equation (5). The polydispersity index (PDI) was calculated with the M_w/M_n ratio.

$$M_w = \frac{\sum (M_i^2 \cdot c_i)}{\sum (M_i \cdot c_i)} \quad \text{Equation 4}$$

$$M_n = \frac{\sum (M_i \cdot c_i)}{\sum c_i} \quad \text{Equation 5}$$

2.6. Colour measurement

The colour of the different alginate extracts was measured using a HunterLab (Color flex, Elscolab) with an aperture of 25 mm. The equipment was calibrated using a green, white and black tile with a 10° standard observer. L*, a* and b* values for each sample were recorded in triplicate.

2.7. Rheological properties of alginate solutions

Rheological properties of the samples were measured using an MCR 302 rheometer (Anton Paar) equipped with a sandblasted parallel-plate (Ø = 25 mm) and a gap size of 1 mm. Aliquots (0.5 ml) of each sample containing 1 % w/v alginate prepared in ultrapure water were loaded into the equipment and allowed to equilibrate for 5 min prior to each measurement. Dynamic viscosity (mPa·s) was measured to determine the rotational shear flow properties over a shear rate range of 1–100 s^{-1} in 41 logarithmic steps. The obtained data over the shear thinning regime was fit to the Ostwald-de Waele power law model (Equation (6)). Where η is dynamic viscosity [mPa·s], K is the consistency index [Pa·s^n], γ is the shear rate [s^{-1}] and n is the flow index [−].

$$\eta = K^* \gamma^{n-1} \quad \text{Equation 6}$$

Strain sweeps were performed to determine the viscoelastic properties of the alginate solutions. The solutions were studied by increasing the strain from 1 to 1000 % under a constant oscillation of 1 Hz in 30 logarithmic steps while recording the storage modulus (G′) and loss modulus (G″). From the test, each measurement was performed in triplicate.

2.8. Texture analysis of calcium alginate gels

Uniaxial compression tests were carried out to evaluate the physical properties of the calcium-induced alginate gels. Gel preparation was based on the protocol described by Farrés (Farrés & Norton, 2014) with modifications. Gels were prepared by mixing a 1 % w/v alginate solution of each sample with enough $CaCO_3$ dispersed in water, followed by the addition of glucono-δ-lactone (GDL) solution. Final concentrations in the samples were 0.5 % w/v, 15 mM and 30 mM of alginate, $CaCO_3$ and GDL, respectively. Mixtures were vortexed vigorously, and 2.4 mL were immediately poured into a 24-well plate with a diameter of 16.28 mm and stored overnight to ensure complete gel formation. The next day, gels were carefully removed from the cylindrical container. A texture analyser (TA.XTplusC, Stable Micro Systems) coupled with a 35 mm diameter aluminium cylinder probe (P/35 Stable Micro Systems) and a 50 kg load cell was used to analyse the samples. Samples were compressed up to 40 % strain at a speed of 1 mm s^{-1}. Equations (7)–(9) were used to calculate the true stress and true strain from the recorded force [N] and distance [mm] data.

$$\varepsilon = -\ln\left(1 - \frac{L - L_0}{L_0}\right) \quad \text{Equation 7}$$

$$A = \frac{A_0}{1 - \varepsilon} \quad \text{Equation 8}$$

$$\sigma = \frac{F}{A} \quad \text{Equation 9}$$

where ε is the true strain [−], calculated from L [mm], the length of the sample, and L_0 [mm], the original sample length; A [mm^2] is the area of the gels during compression and A_0 [mm^2] is the original area of the samples; σ [Pa] is the true stress and F is the recorded force. The Young's modulus, E [Pa], of the different samples was calculated as the slope of the stress-strain curve over the applied deformation. Hardness was defined as the peak force after sample compression. Each measurement was performed in triplicate.

2.9. Statistical analysis

Data analysis was conducted using a one-way ANOVA ($\alpha = 0.05$) to assess statistical differences among the samples. When significant differences were detected, a Tukey's post hoc test was applied to identify pairwise differences. Probability values of $p < 0.05$ were considered statistically significant. All statistical analyses were performed in R-Studio.

3. Results

3.1. DES screening and sequential extraction

A set of different DES were tested for the extraction of alginate from *Saccharina latissima*. Choline chloride-based and betaine-based DES were used, whereas water (H_2O) and the commercially used acid-alkaline (AK) method were used as controls (Fig. 3). The BU extract showed the highest pellet-to-supernatant volume ratio (Figure SM 1). It also resulted in the highest extraction yield among the DES tested (14.9 ± 2.0 %), although this was still lower than the yield obtained with the

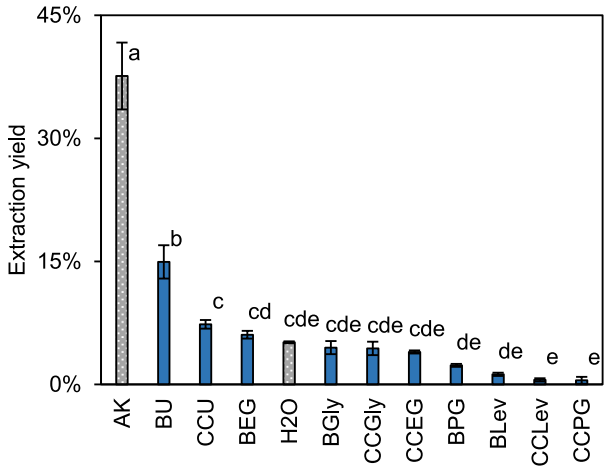

Fig. 3. Extraction yields obtained with different DES and controls (AK and H_2O). Different letters indicate statistically significant differences among groups according to Tukey's test ($p < 0.05$).

acid-alkaline method (37.6 ± 4.1 %). Interestingly, the second-best performer was CCU (7.3 ± 0.5 %), which suggests the potential positive effect of urea on the extraction efficiency. The worst performers were samples containing propylene glycol and levulinic acid as HBD. For the remaining DES, their efficacy under the tested conditions did not surpass that of water (H_2O) alone.

Considering the relatively low yield of the first extraction using DES, a second extraction was performed to further extract the remaining alginate from the residual pellet. Yields of second extractions were registered (Fig. 4). Similarly, as in the previous extraction test, BU performed the best (16.8 ± 1.0 %), followed by CCU (5.7 ± 2.2 %), however, this last was not significantly different from the rest of DES. Similarly to what was observed in the first extraction, samples containing polyols and levulinic acid presented the lowest extraction yields.

To obtain enough alginate for the later characterisation, the extraction was scaled up from 5 g to 200 g of solvent and extraction efficiencies were also measured. The pH values of the processes are provided in Table SM 1 in the supplementary material. Interestingly, the extraction yield from the AK method increased 1.7-fold compared to the extraction efficiency obtained at a smaller scale. On the other hand, marginal increments of the extraction efficiency were observed for BU-1 and BU-2. Importantly, the extraction of a third fraction (BU-3) represented most of the total alginate extracted with BU, with an extraction yield of 38.7 ± 0.04 %. The total alginate extracted with the BU procedure was 75.1 ± 2.2 %, which was higher than the one obtained with the AK method (63.5 ± 1.6 %).

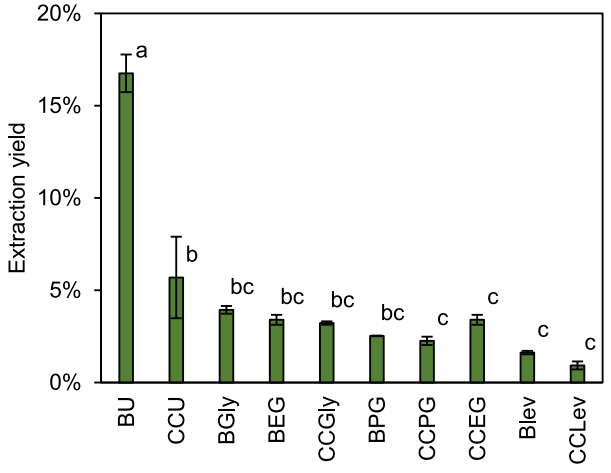

Fig. 4. Extraction yields of the second extraction over the remaining pellet. Different letters indicate statistically significant differences among groups according to Tukey's test ($p < 0.05$).

3.2. Characterisation of extracted alginate

3.2.1. Purity and M/G ratio

The alginate content in the extracts (purity) was determined together with the M/G ratio (Fig. 6). Additionally, other sugars (monosaccharides) were quantified. It was observed that the purity of alginate increased along the sequential BU extractions. The purity obtained for BU-1 was 42.8 ± 1.3 % while for BU-2 and BU-3, purities were 67.2 ± 1.6 % and 73.8 ± 6.3 %, respectively, which presented a purity similar to AK (70.8 ± 4.3 %) ($p < 0.05$). Sugars were also quantified in the samples. Monosaccharides such as fucose, galactose, glucose and mannose were found in relatively relevant amounts, especially in the BU-1, where the total sugars were 11.7 ± 0.7 % (Fig. 7). Among the monosaccharides, fucose was most abundant, especially in BU-1.

In contrast to the purity trend, the M/G ratio decreased from 2.2 ± 0.05 in BU-1 to 1.2 ± 0.05 in BU-3, with BU-2 with a value of 1.5 ± 0.04 (Fig. 6). This downward shift indicates a progressively higher proportion of guluronic units in BU-2 and BU-3. Although relatively lower than the one observed for the AK, there were no statistical differences among the M/G ratios of BU-2, BU-3 and AK ($p < 0.05$).

Purity observed in alginate samples is also correlated with the colour of the alginate solution obtained (Table 3). A more brownish colour was observed in BU-1 and to a lesser extent in BU-2; being BU-3, even clearer than the control AK alginate. This observation is supported by the colour measurements using the L*, a*, b* scale. BU-1 (L* = 18.2; a* = +0.5; b* = +13.2) combines moderate lightness with a strong positive b*, giving a deep, dark-brown tone. BU-2 has higher lightness (L* = 23.8) but a lower b* (+6.9) and a slightly negative a* (−1.3), so the brown weakens to an olive tone. BU-3 is practically achromatic (L* = 9.8; a* ≈ 0; b* ≈ 0), resembling AK, though AK is darker because its lightness is still lower.

3.2.2. Molecular weight

Size exclusion chromatography allowed the determination of *Mw*, *Mn* and PDI from alginate samples (Table 4). AK and BU-1 showed lower *Mw* in comparison to BU-2 and BU-3. Indicating a higher proportion of high molecular weight units. Noticeable is the polydispersity index observed in BU-1, indicating a broad range of molecular sizes in the

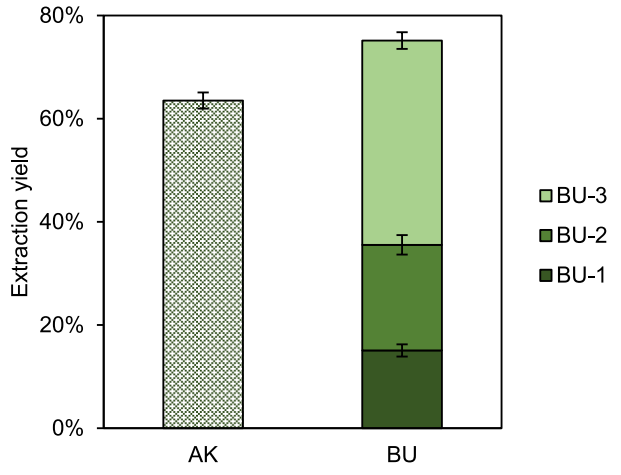

Fig. 5. Extraction yields of the acid-alkaline method and the 3-step BU method.

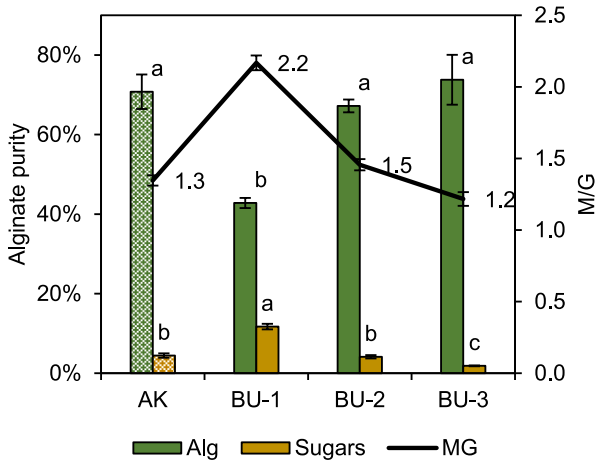

Fig. 6. Purity and M/G ratio of alginate samples. Different letters indicate statistically significant differences among groups according to Tukey's test ($p < 0.05$).

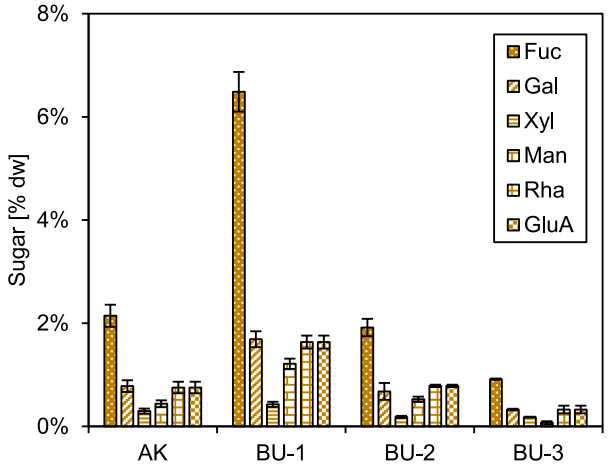

Fig. 7. Monosaccharides in the alginate samples.

sample.

3.2.3. Rheological properties of alginate solutions

The dynamic viscosity of 1 % w/v alginate solutions corresponding to each sample was evaluated, and the viscosity profile within 1 and 100 s^{-1} shear rate was obtained (n = 3) (Fig. 8). Noticeable was the difference between the viscosity profiles of the alginate solutions prepared with the alginate obtained with the AK method, which was at least 2-fold lower (at 10 s^{-1}) than any of the alginate solutions prepared with BU-alginates, being BU-2 and BU-3 being the highest ones. It was observed in all the alginates a shear-thinning behaviour. Noticeable was the viscosity profile of BU-2, which showed a viscosity of 18519 mPa·s at 10 s-1 compared to 1070 mPa·s observed in the AK alginate.

These differences were even more clearly observed when data were fitted to a power law model, and consistency index (*K*) and flow behaviour index (*n*) parameters from each viscosity profile were obtained (Fig. 10). *K* values corresponding to BU-1, BU-2 and BU-3 were higher than the ones obtained for the AK sample. With BU-2 noticeably being the highest with an average value of 105 × 10^3 Pa·s^n, more than 62-fold compared to AK alginate *K*. On the other hand, *n* found for BU-1, BU-2 and BU-3 were far from 1, with values of 0.17 ± 0.05, 0.21 ± 0.01

Table 4
Weight-average molecular weight (*Mw*), number average molecular weight (*Mn*) and polydispersity index. Different superscript letters indicate statistical differences among groups according to Tukey's test ($p < 0.05$).

Sample	Mw [kDa]	Mn [kDa]	PDI
AK	940 ± 23^a	509 ± 14^a	1.9^a
BU-1	918 ± 4^a	292 ± 5^b	3.1^b
BU-2	1159 ± 3^b	640 ± 17^c	1.8^a
BU-3	1230 ± 6^b	773 ± 7^d	1.6^c

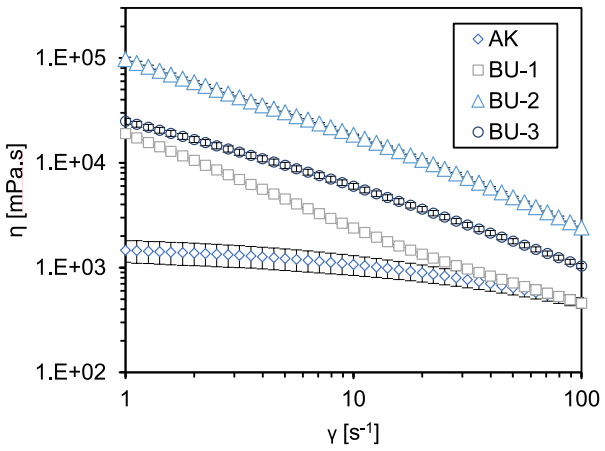

Fig. 8. Flow curves of different alginate extracts at a concentration of 1 % w/v. Data represent the mean of triplicate measurements with standard deviations.

Table 3
Colour measurements (L*, a*, b* scale) of 1 % w/v alginate solutions. From left to right: AK, BU-1, BU-2 and BU-3. Different superscript letters indicate statistical difference among samples ($p < 0.05$) for each colour parameter.

	AK	BU-1	BU-2	BU-3
L*	2.23 ± 0.07^d	18.21 ± 0.03^b	23.79 ± 0.07^a	9.83 ± 0.23^c
a*	−0.62 ± 0.43^b	0.49 ± 0.04^a	−1.3 ± 0.06^c	−0.66 ± 0.09^b
b*	−0.24 ± 0.39^c	13.19 ± 0.08^a	6.87 ± 0.15^b	−0.15 ± 0.17^c
Picture	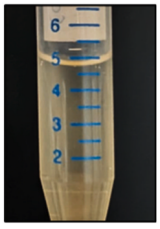	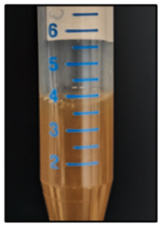		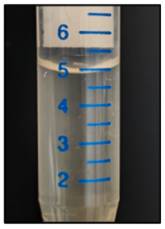

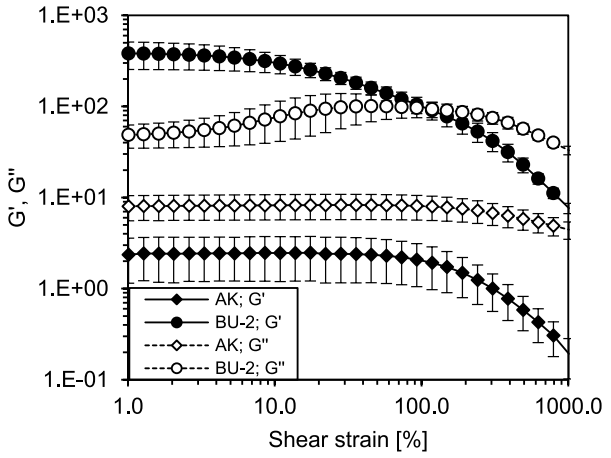

Fig. 9. Amplitude sweep of 1 % w/v of alkaline-extracted alginate solutions (AK) and the second product of BU-DES aided alginate extraction (BU-2). Means are displayed with error bars representing standard deviations of triplicate measurements.

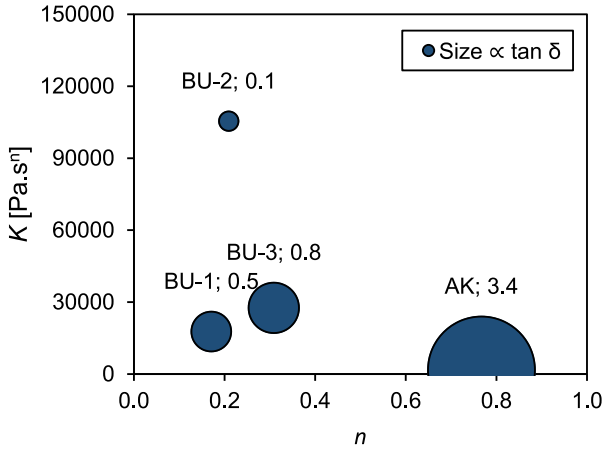

Fig. 10. Consistency index (*K*), flow behaviour index (*n*) and loss factor (*tan* δ at 1 % shear strain). The loss factor is represented by the size of the marker. For clarity, error bars are not displayed, although means and standard deviation are shown in Table SM 2.

and 0.31 ± 0.01, respectively, contrary to what was observed in the case of the AK alginate, whose value was 0.77 ± 0.04.

The storage modulus (G′) and loss modulus (G″) of alginate samples were obtained from amplitude sweep tests. For clarity, only data from AK and BU-2 are presented in Fig. 9, while the remaining data for BU-1 and BU-3 are available in the supplementary material in Figure SM 3. For the AK sample, G′ remained lower than G″ across the entire tested shear strain range, indicating a predominantly viscous behaviour. In contrast, BU-2 exhibited G′ values significantly higher than G″, suggesting a more elastic response. However, this trend reversed when shear strain exceeded 100 %, indicating a transition where G″ became dominant. In Fig. 10, the G'/G'' (*tan* δ) is expressed as the inverse of the circle size. From this Figure it can be observed that samples with lower flow behaviour indexes (*n*) also presented lower *tan* δ values, highlighting the differences in the viscous behaviour of BU-extracted alginate compared to the acid-alkaline control.

3.2.4. Physical properties of calcium-induced alginate gels

Gels were prepared containing 0.5 % w/v alginate with calcium. Those gels were compressed in a Texture Analyser, and hardness [g] and Young's modulus *E* [Pa] were obtained (Fig. 11). AK, BU-2 and BU-3 showed similar hardness values. The hardness observed in the BU-1 was less than half that of the one observed in AK alginate and the other two BU alginates. ($p < 0.05$) A similar pattern was observed regarding the Young's modulus values. The *E* value from BU-2 (6488 ± 300 Pa) was comparable with AK (6353 ± 166 Pa) and BU-3 (6028 ± 197 Pa). BU-1 again showed the lowest Young's modulus (3138 ± 39 Pa) ($p < 0.05$).

4. Discussion

4.1. Alginate extraction with deep eutectic solvents

The successful extraction of alginate is linked to the effectiveness of cell wall degradation and later solubilization of alginate without the interference of divalent cations that are originally linked to the alginate. When the conventional acid-alkaline extraction is performed, one of the main roles of the acid treatment is to partially break down the tough cell wall structure, freeing the alginate that is embedded in it (Draget, 2009; Rahman et al., 2024; Saji et al., 2022).

Among all choline chloride- and betaine-based DES, only the BU stands out among the rest, although with a much lower yield compared with the acid-alkaline (AK) method. Evidently, optimisation of the extraction process is necessary, as temperature and time may significantly influence the outcome. This is especially important considering the relatively higher viscosity of DES compared to aqueous solutions (Al Fuhaid et al., 2023), which can hinder mass transfer and reduce extraction efficiency. This factor, along with the increased viscosity caused by the presence of extracted alginate, may have affected the subsequent extraction of additional alginate. Interestingly, the second-best performer for alginate extraction was CCU. It is worth noting that CCU was the top performer among a group of choline chloride-based DES screened by Hiemstra et al. (2024), although its alginate techno-functional properties were not evaluated.

Interestingly, after the first extraction, the residual pellet from betaine-based DES appeared swollen (Figure SM 1), particularly noticeable in the case of BU. This observation suggested that structural changes may have occurred in the seaweed matrix. Moreover, when a second extraction was performed using only water, BU remained the best-performing system. In contrast to the other DES, which yielded no

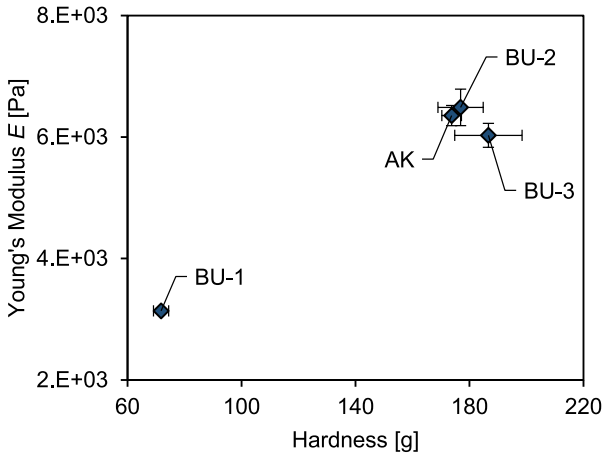

Fig. 11. Hardness and Young's modulus *E* obtained from calcium-induced gels of different alginate extracts. Data displays the mean of triplicate samples with standard deviations.

more than an additional 5 %, BU enabled the extraction of approximately 17 % more alginate in the second step. This relatively high extraction yield may be explained by a change in osmotic equilibrium, potentially generating a pressure gradient strong enough to disrupt the seaweed cell structure, thereby facilitating the second extraction.

Betaine is a compound well-known for its properties as an osmolyte, i.e. plays a crucial role in regulating osmotic pressure (Cayley & Record, 2003; Lever & Slow, 2010; Natalello et al., 2009). Also known as trimethylglycine, betaine is a zwitterionic compound containing both negative and positive charges, which together form an inner salt (Al Fuhaid et al., 2023; Jiang & Zheng, 2023; Nava-Ocampo et al., 2021). However, the positive charge is partially shielded by methyl groups, making betaine a relatively poor cation but a good hydrogen bond acceptor (HBA) (Abranches et al., 2020, pp. 4916–4921). Given that alginate contains abundant hydroxyl and carboxyl groups, strong hydrogen bonding can occur between alginate and betaine, potentially contributing to the stabilisation of alginate structures. Indeed, previous studies have reported strong hydrogen-bond networks between betaine and alginate, which have also been applied in cryoprotection (J. Yang et al., 2019a).

In the context of this work, the hypertonic conditions generated during contact with the betaine-urea (BU) system may have promoted water transfer from the hydrated seaweed into the BU phase, potentially displacing cell membranes and disrupting the cell wall structure. Simultaneously, BU components may have diffused into the cellular matrix, establishing a new equilibrium and dissolving cytoplasmic components. Although the diffusion of osmolytes such as betaine typically requires specific transport proteins (Ressl et al., 2009), drying processes, including freeze-drying, are known to alter membrane permeability (Neoh et al., 2016; Rockinger et al., 2021; Silva et al., 2019), likely facilitating the passive diffusion of betaine into the cells. Once inside, betaine (and urea) may have interacted directly with water-binding polysaccharides such as alginate, enhancing the hydrogen-bond network between alginate, betaine, and water. This could explain the higher water retention observed within the cell wall matrix, manifested as swollen biomass. Additionally, it has been suggested that highly hydrated DESs, as occurred during the second extraction, may further promote cell wall distortion (T. X. Yang et al., 2017), which may have also contributed to the observed extraction enhancement in the second extraction step.

Osmotic shocks have been reported as suitable techniques for cell disruption and inner components recovery, such as lipids from microalgae (González-gonzález et al., 2019; Halim et al., 2021). Additionally, protein extraction yields were improved when using this technique in *Saccharina latissima* (Veide Vilg & Undeland, 2017). Postma et al. (2018) found this technique to be effective, although with long periods of treatment.

The reader will notice that despite the presence of betaine as HBA in combination with other HBD such as ethylene glycol, propylene glycol, glycerol and levulinic acid, their corresponding yields were much lower in comparison with urea. Then, indicating a synergistic effect among betaine and urea, a synergy that was explored by Zeng et al. (2016).

The hypothesis of BU working as a disruption pretreatment is further supported by the extraction yield obtained in the third extraction step, where sodium carbonate was added (pH 10–11), resulting in BU-3. Interestingly, the EY was much higher than the previous steps (~36.9 %). In total, the extraction yield (~72.5 %) of the whole process using BU was higher compared to the conventional method (~63.5 %). The sequential extraction process proposed with BU involves one additional step, but it can be carried out without the need for acid pretreatment, unlike the conventional acid–alkaline method. Evidently, if only one extraction step is desired, the optimisation of one of them (preferably the aqueous one) should be performed. This represents a potential mild disruption method and might allow the release of less degraded alginate.

4.2. BU-alginate characterisation

4.2.1. Purity and colour

Alginate purity is an important parameter depending on the application, being the pharmaceutical application being the most strict one (Fu et al., 2011; Yong & Mooney, 2012). Achieving a high purity is not always easily accomplished, as during the extraction process, other compounds present in the seaweed can be co-extracted. Then, the different (pre-) treatments are oriented to remove undesired compounds. The acidification step aims to remove divalent cations and degrade easily degradable polysaccharides, such as fucoidans, with the extent of removal depending on the efficiency of this step (Saji et al., 2022). Residual fucose and other sugars were detected in the AK alginate, although, as expected, in relatively small amounts (less than 5 %). If fucoidan is in high amounts, methods of separation such as dialysis, as used in this research work (3.5 kDa cutoff), would have been insufficient, as the molecular weight of fucoidan is within the range of alginate molecular weight (Gómez-Ordóñez et al., 2012; Rupérez et al., 2002). Additionally, ethanol precipitation, used to recover alginate, can also precipitate fucoidan (Lim et al., 2017). The presence of impurities indicated by the relatively higher level of fucose and other monosaccharides such as galactose (summing a value of ~11.7 % on a dry basis) was noticeable in BU-1, suggesting a coextraction of fucoidan together with alginate. This was not the case on BU-2 alginate and BU-3 alginate, where sugars were present in less than 5 % and 2 %, respectively. Fucoidan is known for its hydrophilic nature, largely attributed to its ionic character resulting from the presence of sulphate groups. Hot water is generally sufficient to extract significant amounts of this sulphated fucose-rich polysaccharide (Lim et al., 2017; Zayed et al., 2020). Given the relatively low fucoidan content in Saccharina latissima (~4–6 % dry basis) compared to alginate (Bruhn et al., 2017) and the highly hydrogen-bonding environment created by betaine-urea-water DES (Abranches et al., 2020, pp. 4916–4921), it is reasonable to assume that the majority was extracted during the initial extraction step (BU-1). This would explain the marginal amounts detected in the subsequent fractions (BU-2 and BU-3). The aforementioned findings are supported by Fourier Transform Infrared (FT-IR) spectroscopy analysis (Figure SM 4), which is presented in the Supplementary Material.

Besides sugars, the presence of impurities in BU-1 was also evident from the colour of the alginate solution, which was less pronounced in BU-2 and negligible in BU-3 (Table 3). In fact, BU-1 alginate showed a very brownish colour. One very probable reason is the presence of fucoxanthin, which possesses certain hydrophilicity due to its slight polarity (Kholany et al., 2025) that might have allowed its partition into BU, although its hydrophobicity is dominant. Despite its dominant hydrophobicity, one phenomenon that might have played a role in the coextraction of fucoxanthin in the first step is the hydrotropic behaviour of betaine. A hydrotrope is a molecule that enhances the solubility of hydrophobic compounds in hydrophilic media. Zwitterionic compounds, such as betaine, are among those capable of exhibiting hydrotropic behaviour (Patel & Desai, 2023). In fact, in the presence of water, betaine exhibits amphiphilic character, potentially allowing the dissolution of more apolar compounds such as fucoxanthin (Di Gioacchino et al., 2020).

The brownish colour could also come from the oxidised polyphenols, also known as phlorotannins, present in relevant amounts in brown seaweed (Sardari et al., 2021). These are normally removed via formalin usage as a pretreatment (Boussetta et al., 2021; Saji et al., 2022), a step that was skipped in this research work. Additionally, phlorotannins are difficult to remove via dialysis as their molecular weight falls within the alginate range (Kwon et al., 2023). Those polyphenolic compounds could have been oxidised during the extraction process, creating a darker colour (Gisbert et al., 2022; Montes et al., 2021). Finally, phlorotannins covalently bond to proteins (Stern et al., 1996) present in seaweed might have precipitated together with alginate, intensifying the darker colour.

4.2.2. Rheology and chemistry of extracted alginate

4.2.2.1. Alginate solutions. Alginate is extensively used across different industries due to its high viscosity in solution and straightforward gel formation. Those characteristics are closely linked to factors such as substrate species, extraction method, isolation method and ions present in the alginate solution (Saji et al., 2022). The severity of the pretreatment, which is always linked to seaweed cell wall toughness, also determines the chemical properties of the alginate, such as the MG ratio and the molecular mass of the polysaccharide. These parameters define the potential applications of the polymer (Draget, 2009; Draget et al., 1994).

Rheological parameters of 1 % w/v solutions prepared with the obtained alginate were evaluated. Importantly, alginate fractions showed a non-Newtonian shear-thinning behaviour, typically observed in sodium alginate solutions (Ma et al., 2014). All alginates obtained from the extraction using BU showed a higher consistency index (*K*) (a parameter related to viscosity for non-Newtonian fluids), compared with the AK sample (Fig. 10), indicating a greater resistance to flow. Similar behaviour was observed by Moradiya and Pereira (2024), who used choline chloride glycolic acid DES as an extraction solvent.

The viscosity of alginate solutions is a function, among others, of the molecular weight of the polysaccharide chains (Draget, 2009; Neves et al., 2020). Polymeric solutions such as alginate commonly present 4 different concentration regimes, namely, the diluted, the semi-dilute unentangled, the semi-dilute entangled, and the concentrated (Dodero et al., 2019). At low concentration, alginate chains are isolated from each other with minimal interaction. When concentration increases, chains begin to overlap, although without entanglements. At much higher concentrations, chain entanglement occurs, creating a continuous network. Being alginate a polyelectrolyte, the viscosity increases even more due to the electrostatic repulsion between negatively charged chains (Dodero et al., 2019). This relation is determined by the Mark-Houwink relation (Equation (3)) (Draget et al., 1994; Haug & Smidsrød, 1962; Holme et al., 2003, 2008). This equation indicates that the higher the molecular weight, the higher the viscosity of the solution prepared with that alginate.

While the *Mw* of BU-2 and BU-3 alginates were significantly higher than the acid-alkaline control (AK), this was not the case for BU-1. Interestingly, although the *Mw* of BU-1 was similar to that of AK, the PDI of BU-1 was considerably higher, suggesting a broader molecular weight distribution with the presence of low-molecular-weight chains, which would typically be expected to reduce the solution viscosity. However, the experimental data contradicts this expectation, as BU-1 exhibited a *K* value approximately 10 times higher than that of AK-extracted alginate (Fig. 10). Similarly, the *Mw* of BU-2 and BU-3 were higher than AK, although they had similar PDI. However, the *K* index exhibited by BU-2 was 62-fold AK sample (Fig. 10). Although the viscosity of alginate solutions increases exponentially with the *Mw* (as described by the Mark-Houwink relation), this was not the case for BU-1.

The severity of acid–alkaline conditions strongly affects alginate *Mw*. In the AK sample, acidification with 0.2 M H_2SO_4 (pH 1.9) for 1 h likely caused partial depolymerisation (Gomez et al., 2009), explaining its lower *Mw* compared to BU-2 and BU-3. Although BU-1 had a similar *Mw* to AK, its higher polydispersity index (PDI) reflects a wider range of chain lengths. BU-1 yielded only 15.1 % of total extractable alginate (vs. 63.5 % for AK) (Fig. 5), indicating preferential solubilization of shorter chains, while longer chains remained for later extraction. The high PDI observed in BU-1 may have resulted from the extraction of more exposed and labile mannuronic acid-rich (M-rich) regions (Aida et al., 2010, 2022) under the slightly alkaline conditions of BU-DES (apparent pH ~9.0), as guluronic acid (G) blocks are more tightly bound to divalent cations (Cao el al., 2020). Additionally, partial degradation of alginate may have occurred prior to extraction due to endogenous alginate lyase activity from the seaweed or associated marine microbiota (Zhu & Yin, 2015).

The discrepancy observed in BU-1 regarding the *Mw* and the viscosity suggests the simultaneous occurrence of an additional phenomenon. One possibility is that BU-1, having a higher prevalence of charged groups, might have favoured stronger interactions with the medium and thereby increased its viscosity. Alternatively, interactions with residual betaine-urea may have also contributed to this behaviour.

Fig. 9 shows the storage and loss moduli (G′ and G″, respectively) for AK and BU-2. The G′ value for BU-2 is an order of magnitude higher than that of AK, indicating a much stiffer material, in contrast to the predominantly viscous behaviour observed for AK (Norton et al., 2011). The low flow index of BU-2 ($n \approx 0.21$) and the high consistency index ($K \approx 1 \times 10^5$ Pa·s^n) (Fig. 10) are consistent with the elastic dominance observed in Fig. 9. The ratio of G″ over G′ (also known as *tan δ*) is an indication of the rheological behaviour of the materials. When G′> G″, the material behaves more like a solid exhibiting elasticity; otherwise, the material shows more a viscous behaviour, i.e. liquid-like (Farrés & Norton, 2014; Ma et al., 2014; Norton et al., 2011). Interestingly, and contrary to what Moradiya and Pereira (2024) observed, the *tan δ* of BU-2 was below 1 for a wide range of shear strain evaluated (Fig. 10), confirming a more elastic behaviour of this alginate (Norton et al., 2011). This was not necessarily true for BU-3, in which, while still predominantly elastic, the *tan δ* was closer to 1. Considering that no calcium was added, the high viscosity and elastic behaviour observed in BU-2 may be explained by the residual presence of DES components, similar to BU-1, which could have promoted extensive hydrogen bonding along the long-chain (high *Mw*) alginates.

It is tempting to speculate that, due to its ionic nature (Fernando et al., 2019; Lim et al., 2017), fucoidan, particularly in BU-1, may have contributed to the observed increase in viscosity. Fucoidan itself is not a thickening agent and exhibits low viscosity in solutions (Zayed et al., 2020), although, as it was mentioned before, its molecular weight ranges within the alginate (Gómez-Ordóñez et al., 2012; Rupérez et al., 2002; Sweeney & O'Doherty, 2016). Additionally, fucoidan can exhibit both linear and branched structures and may contain a variety of residues attached to its backbone (Moreira et al., 2023). Brovko et al. (2023) studied the physicochemical properties of sodium alginate-fucoidan mixtures and suggested a strong interaction via hydrogen bonding. Although they observed a reduction in the viscosity as the fraction of fucoidan increased in the mixture. A positive effect of fucoidan on the rheological properties of mixtures with other polysaccharides has been observed; however, this effect was reported to be limited and, in some cases, even to nullify the expected synergistic behaviour (Bak & Yoo, 2024; Zheng et al., 2022). Therefore, it is very likely that betaine played a significant role in the observed increase in viscosity and elastic behaviour. As previously discussed, betaine has a strong affinity for both alginate and water (J. Yang et al., 2019b). Its presence may have promoted a certain degree of ionic crosslinking between alginate molecules (Fernando et al., 2019), contributing to the formation of a stable and robust three-dimensional network. This network, reinforced by multiple hydrogen-bonding points, could explain the increased viscosity and enhanced elastic behaviour observed in BU-2.

4.2.2.2. Calcium-induced alginate gels. Similarly to its behaviour in solution elaborated in the previous section, the gelling properties of alginate in the presence of calcium are also of significant importance (Farrés & Norton, 2014; Roopa & Bhattacharya, 2008). One of the most common methods to form alginate gels is by incorporating divalent ions, with calcium (typically added as calcium chloride) being the most widely used (Larsen et al., 2015). Calcium binds to the alginate through specific regions rich in guluronate units, forming three-dimensional networks described by the "egg-box" model (Larsen et al., 2015; Rinaudo, 2007). Therefore, a higher guluronate content (i.e., a lower M/G ratio) provides more binding sites, resulting in a more rigid gel structure.

The BU alginates exhibited varying M/G ratios. BU-1 had the lowest ratio (2.2), while BU-2 (1.5) and BU-3 (1.2) showed values closer to that of the AK sample (1.3). As expected. These M/G ratios correlated inversely with the gel hardness measured by texture profile analysis (TPA) of the calcium alginate gels. Interestingly, there was no apparent effect of the betaine-urea presence on the calcium-gelling properties of extracted alginate. BU-2, BU-3, and AK gels exhibited similar hardness levels, with no significant differences observed ($p > 0.05$). Similarly, Young's modulus was only different in the BU-1 calcium gel ($p < 0.05$) network.

Calcium-alginate gel hardness and Young's modulus are only marginally altered by the BU extraction steps, in marked contrast to the pronounced rise in solution viscosity. This divergence again suggests that the viscosity increase could originate from strengthened alginate-–alginate associations, potentially amplified by residual betaine-urea. In contrast, the gel mechanical properties remain mainly dictated by calcium selective binding to guluronic-acid blocks. Consequently, the alginate M/G ratio continues to be the principal factor governing stiffness and hardness across all calcium-cross-linked systems examined.

It could be interesting to note the trend of M/G observed among BU samples. Data suggest that M-rich alginates (as indicated by the M/G ratio of 2.2 in BU-1) are more accessible during the initial stages of extraction. This is consistent with previous reports indicating that M-rich alginates tend to be more flexible and more easily hydrated compared to alginates with lower M/G ratios. (Qosim et al., 2024). Likely, M-rich alginate dissolves more readily than G-rich alginate, which is subsequently released, likely aided by BU-DES.

Divalent cations, such as Ca^{2+}, are naturally present in brown seaweed. They contribute to the formation of the so-called "egg-box" model, in which they are strongly bound to guluronic acid units, creating cross-links within the alginate matrix (Draget, 2009; Rinaudo, 2007). During the first betaine-urea DES extraction (BU-1), the solvent acts as a powerful hydrogen bond acceptor (Abranches et al., 2020), yet provides no chelation effect. Thus, it dissolves mainly non-crosslinked, flexible MM and MG regions while Ca-GG regions remain mostly intact. This yields a swollen residue and the highest M/G ratio (2.2). When DES is diluted with water (BU-2), its viscosity falls and the polarity rises due to strong interactions with water (Abranches et al., 2020, 2021), accelerating the diffusion of already exposed chains. Mixed MG and GG sections are now released, lowering the M/G ratio to 1.5. In the final sodium carbonate step (BU-3), CO_3^{2-} ions sequester the residual Ca^{2+}, and the excess Na^+ promotes the formation of soluble sodium alginate, freeing the calcium-locked G-rich fibres and producing the lowest M/G ratio observed (1.2).

4.2.2.3. Perspectives. The rheological properties of alginate extracted using BU highlight its potential for food applications requiring high-viscosity hydrocolloids, such as sauces, dressings, or plant-based dairy alternatives. In addition, sectors such as the medical field demand this type of material, and alginate has already demonstrated its suitability for various applications (Neves et al., 2020; Storz et al., 2009). Furthermore, the gathered results on the physical properties of the calcium-induced gels show that it is possible to extract alginate through a sequential BU extraction, having similar gelling properties as alkali-extracted alginate. Nevertheless, further molecular-level studies, using techniques such as NMR, could provide deeper insights into the influence of betaine–urea on the rheological behaviour of these alginates. Additionally, process optimisation is still needed to reduce the number of extraction steps, ideally limiting it to two. This could be achieved by redesigning the first extraction as a pretreatment, fine-tuning the process parameters or de DES composition, followed by an optimised diluted BU extraction. Such an approach would simplify the process while maintaining the production of alginate with desirable rheological properties.

Beyond the techno-functional properties of the extracted alginate, potential toxicity from residual solvents may limit its applicability in certain end uses. However, the amount of residual DES in the final alginate product is expected to be minimal for several reasons. Following extraction, the DES-alginate solution is dialysed using a 3.5 kDa cutoff membrane, a step in which most DES components are expected to diffuse out. The resulting alginate-containing solution is then precipitated with ethanol (80 % v/v + 1 % NaCl) and washed twice with 80 % ethanol. This sequence is expected to effectively remove residual betaine and urea from the alginate fraction (House & House, 2017; Wang, Qin, Zhou, & Wang, 2012). Moreover, betaine intake has been deemed safe up to 6 mg/kg body weight per day (Turck et al., 2019) and urea is classified as GRAS (Generally Recognised As Safe) by theU.S. Food and Drug Administration (2025). Assuming a hypothetical 1 % (w/w) residual DES content in the alginate, a 70 kg person would need to consume approximately 42 g of alginate per day to reach the safety limit for betaine, an intake far exceeding conventional consumption levels. Furthermore, cytotoxicity studies using BU-DES on human skin cells have shown low toxicity, indicating a favourable biocompatibility profile (Olivares et al., 2022). Taken together, the anticipated low levels of DES residue, combined with regulatory thresholds and existing toxicological data, suggest minimal risk associated with residual DES in the final product. Nevertheless, long-term and chronic exposure studies remain necessary to fully establish the safety profile.

It is important to emphasise the need to develop sustainable processes for seaweed biomass valorisation. In this context, the recovery and reusability of DES components should be further explored. Moreover, reducing or eliminating the use of ethanol at an industrial scale would significantly improve the environmental footprint of the process. For alginate separation, alternative methods such as membrane filtration, as proposed by Elizondo et al. (2024), offer promising, solvent-free options. Following filtration, the permeate, composed primarily of betaine, urea, and other low molecular weight compounds, can potentially be restored to its original composition through techniques such as vacuum evaporation, allowing water content to be adjusted as needed (Algieri et al., 2024; Li, 2022). To further enhance both the sustainability and economic viability of the process, the recovery of additional valuable compounds, such as fucoidan from the first extracted fraction (BU-1), whose co-extraction with alginate is suggested by the relatively high monosaccharide content (Fig. 7), should also be considered. This integrated strategy would support the development of a true multi-product seaweed biorefinery. Finally, future research should include techno-economic analysis and life cycle assessment to provide a comprehensive evaluation of the process and its industrial feasibility.

5. Conclusions and recommendations

This study evaluated the extraction of alginate using choline chloride- and betaine-based DES, each combined with one of five hydrogen bond donors: urea, ethylene glycol, propylene glycol, glycerol, and levulinic acid. Among these, the betaine-urea DES (BU) at a 1:2 M ratio with 10 % water showed the highest extraction performance. Further sequential aqueous and alkaline extractions suggested that BU not only dissolves alginate effectively but may also play a disruptive role in the seaweed structure. The cumulative alginate yield using BU (75.1 ± 2.2 %) was higher compared to that obtained with conventional acid-alkaline extraction (63.5 ± 1.6 %).

Three alginate fractions (BU-1, BU-2 and BU-3) were obtained from the sequential BU extraction and analysed for their chemical and rheological properties. All exhibited shear-thinning behaviour and higher apparent viscosities at low shear rates compared to the acid-alkaline (AK) control. BU-2 stood out with a consistency index (K) 62 times greater than AK and showed elastic behaviour ($tan\ \delta < 1$), in contrast to the liquid-like behaviour of AK ($tan\ \delta > 1$). Molecular weight analysis revealed higher fractions of high-molecular-weight alginate in BU-2 and BU-3, suggesting lower depolymerisation and indicating a milder disruptive effect by BU compared to acid-alkali extracted alginate. The

higher viscosity at low shear rates displayed by BU-1, despite having a similar average molecular weight, suggests that betaine-urea might have played a role in the enhanced rheological properties of alginate. On the other hand, BU-1 presented lower compression strength of calcium-induced gels compared to BU-2 and BU-3, which were similar to AK alginate. As expected, gel strength correlated inversely with MG ratio, indicating that a sequential BU-DES extraction can be used to selectively produce alginate fractions with varying MG composition.

Overall, this study provides valuable insights into the interaction between DES and seaweed biomass, particularly how DES-based extraction influences seaweed structure and alginate properties. BU-extracted alginates exhibited notable differences compared to conventionally extracted samples. Differences likely arose from the milder conditions and specific interactions between BU components and alginate. These findings open new possibilities for producing alginate with tailored properties for niche applications in food, pharmaceuticals, and materials science.

CRediT authorship contribution statement

Wimar Reynaga-Navarro: Writing – original draft, Methodology, Investigation, Formal analysis, Conceptualization. **Lucas Bozzo:** Writing – review & editing, Methodology, Formal analysis. **René H. Wijffels:** Writing – review & editing. **Michel Eppink:** Writing – review & editing. **Antoinette Kazbar:** Writing – review & editing, Supervision, Project administration, Funding acquisition, Conceptualization.

Authors statement

Wimar Reynaga Navarro: Conceptualisation, methodology, investigation, formal analysis and writing of the original draft. Lucas Bozzo: Methodology, formal analysis, and writing-reviewing and editing. Rene Wijffels: writing-reviewing and editing. Michel Eppink: writing-reviewing and editing. Antoinette Kazbar: Conceptualisation, writing-reviewing and editing, supervision, project administration and funding acquisition.

Declaration of generative AI and AI-assisted technologies

During the preparation of this manuscript the authors used ChatGPT-4o (OpenAI) solely to improve the grammar and readability ot the text. After using this tool, the authors reviewed and edited the content as needed and take full responsibility for the content of the published article.

Declaration of competing interest

The authors declare that they have no known competing financial interests or personal relationships that could have appeared to influence the work reported in this paper.

Acknowledgements

This research work was funded by the Dutch Research Council (NWO) https://app.dimensions.ai/details/grant/grant.12924032. Grant number:19479.

Appendix A. Supplementary data

Supplementary data to this article can be found online at https://doi.org/10.1016/j.foodhyd.2025.111862.

Data availability

Data will be made available on request.

References

Abasalizadeh, F., Moghaddam, S. V., Alizadeh, E., Akbari, E., Kashani, E., Fazljou, S. M. B., Torbati, M., & Akbarzadeh, A. (2020). Alginate-based hydrogels as drug delivery vehicles in cancer treatment and their applications in wound dressing and 3D bioprinting. *Journal of Biological Engineering, 14*(1), 17. https://doi.org/10.1186/s13036-020-00239-0

Abbott, A. P., Capper, G., Davies, D. L., Rasheed, R. K., & Tambyrajah, V. (2003). Novel solvent properties of choline chloride/urea mixtures. *Chemical Communications, 1*, 70–71. https://doi.org/10.1039/b210714g

Abranches, D. O., Silva, L. P., Martins, M. A. R., & Coutinho, J. A. P. (2021). Differences on the impact of water on the deep eutectic solvents betaine/urea and choline/urea. *Journal of Chemical Physics, 155*(3). https://doi.org/10.1063/5.0052303

Abranches, D. O., Silva, L. P., Martins, M. A. R., & Pinho, S. P. (2020). *Understanding the formation of deep eutectic solvents : Betaine as a universal hydrogen bond acceptor*. https://doi.org/10.1002/cssc.202001331

Agilent Technologies Inc. (2015). *Polymer molecular weight distribution and definitions of MW averages technical overview number average molecular weight : Mn*.

Aida, T. M., Kumagai, Y., & Smith, R. L. (2022). Mechanism of selective hydrolysis of alginates under hydrothermal conditions. *Journal of Bioresources and Bioproducts, 7*(3), 173–179. https://doi.org/10.1016/j.jobab.2022.04.001.

Aida, T. M., Yamagata, T., Watanabe, M., & Smith, R. L. (2010). Depolymerization of sodium alginate under hydrothermal conditions. *Carbohydrate Polymers, 80*(1), 296–302. https://doi.org/10.1016/j.carbpol.2009.11.032.

Al Fuhaid, L., Nava-Ocampo, M. F., Bucs, S. S., Verpoorte, R., Choi, Y. H., Witkamp, G. J., & Farinha, A. S. F. (2023). Crystallization and time-dependent changes in betaine-urea-water natural deep eutectic solvents. *Journal of Molecular Liquids, 387*. https://doi.org/10.1016/j.molliq.2023.122718

Alcalde, R., Aguilar, N., Escobedo-Monge, M. A., Trenzado, J. L., Atilhan, M., Bol, A., & Aparicio, S. (2024). On the properties of water in betaine – Based deep eutectic solvents. *Journal of Molecular Liquids, 406*. https://doi.org/10.1016/j.molliq.2024.124871

Algieri, V., Maiuolo, L., Procopio, D., Costanzo, P., Nicoletta, F. P., Trombino, S., … Nino, A. De.. Reactive deep eutectic solvent for an eco-friendly synthesis of cellulose carbamate. https://doi.org/10.3390/polym16060757.

Aroso, I. M., Paiva, A., Reis, R. L., & Duarte, A. R. C. (2017). Natural deep eutectic solvents from choline chloride and betaine – Physicochemical properties. *Journal of Molecular Liquids, 241*, 654–661. https://doi.org/10.1016/j.molliq.2017.06.051

Bak, J., & Yoo, B. (2024). Effect of fucoidan on conformation of xanthan gum and its tribo-rheological properties. *Biomacromolecules, 25*(11), 7274–7282. https://doi.org/10.1021/acs.biomac.4c00973

Bojorges, H., López-Rubio, A., Fabra, M. J., & Martínez-Abad, A. (2023). Estimation of alginate purity and M/G ratio by methanolysis coupled with anion exchange chromatography. *Carbohydrate Polymers, 321*(July), Article 121285. https://doi.org/10.1016/j.carbpol.2023.121285

Bojorges, H., López-Rubio, A., Martínez-Abad, A., & Fabra, M. J. (2023). Overview of alginate extraction processes: Impact on alginate molecular structure and techno-functional properties. *Trends in Food Science & Technology, 140*(May). https://doi.org/10.1016/j.tifs.2023.104142

Boussetta, A., Ablouh, E. H., Benhamou, A. A., Taourirte, M., & Moubarik, A. (2021). Valorization of Moroccan brown seaweeds: Elaboration of formaldehyde-free particleboards based on sodium alginate–corn-starch - Mimosa tannin wood adhesives. *International Journal of Adhesion and Adhesives, 108*. https://doi.org/10.1016/j.ijadhadh.2021.102894

Brovko, O., Palamarchuk, I., Gorshkova, N., & Bogolitsyn, K. (2023). Physicochemical properties and compatibility of sodium alginate and fucoidan solutions. *International Journal of Biological Macromolecules, 243*(March), Article 125309. https://doi.org/10.1016/j.ijbiomac.2023.125309

Bruhn, A., Janicek, T., Manns, D., Nielsen, M. M., Balsby, T. J. S., Meyer, A. S., … Bjerre, A. B. (2017). Crude fucoidan content in two North Atlantic kelp species, Saccharina latissima and Laminaria digitata—seasonal variation and impact of environmental factors. *Journal of Applied Phycology, 29*(6), 3121–3137. https://doi.org/10.1007/s10811-017-1204-5.

Cao, L., Lu, W., Mata, A., Nishinari, K., & Fang, Y. (2020). Egg-box model-based gelation of alginate and pectin : A review. *Carbohydrate Polymers, 242*(April), 116389. https://doi.org/10.1016/j.carbpol.2020.116389.

Cayley, S., & Record, M. T. (2003). Roles of cytoplasmic osmolytes, water, and crowding in the response of Escherichia coli to osmotic stress: Biophysical basis of osmoprotection by glycine betaine. *Biochemistry, 42*(43), 12596–12609. https://doi.org/10.1021/bi0347297

Cesaretti, M., Luppi, E., Maccari, F., & Volpi, N. (2003). A 96-well assay for uronic acid carbazole reaction. *Carbohydrate Polymers, 54*(1), 59–61. https://doi.org/10.1016/S0144-8617(03)00144-9

Das, A. K., Sharma, M., Mondal, D., & Prasad, K. (2016). Deep eutectic solvents as efficient solvent system for the extraction of κ-carrageenan from Kappaphycus alvarezii. *Carbohydrate Polymers, 136*, 930–935. https://doi.org/10.1016/j.carbpol.2015.09.114

de Souza Mesquita, L. M. (2024). The perfect match between macroalgae and eutectic solvents as a sustainable gateway to ready-to-use extracts towards a (blue + green) economy — A perspective review. In *Bioresource technology, 414*. Elsevier Ltd. https://doi.org/10.1016/j.biortech.2024.131600

Deniaud-Bouët, E., Kervarec, N., Michel, G., Tonon, T., Kloareg, B., & Hervé, C. (2014). Chemical and enzymatic fractionation of cell walls from fucales: Insights into the structure of the extracellular matrix of brown algae. *Annals of Botany, 114*(6), 1203–1216. https://doi.org/10.1093/aob/mcu096

Di Gioacchino, M., Bruni, F., & Ricci, M. A. (2020). Aqueous solution of betaine: Hydration and aggregation. *Journal of Molecular Liquids, 318*. https://doi.org/10.1016/j.molliq.2020.114253

Dodero, A., Vicini, S., Alloisio, M., & Castellano, M. (2019). Sodium alginate solutions: Correlation between rheological properties and spinnability. *Journal of Materials Science, 54*(10), 8034–8046. https://doi.org/10.1007/s10853-019-03446-3

Draget, K. I. (2009). Alginates. In *Handbook of hydrocolloids* (pp. 807–828). Elsevier. https://doi.org/10.1533/9781845695873.807.

Draget, K. I., Br, G. S., & Smidsrod, O. (1994). *Alginic acid gels : The effect of alginate chemical composition and molecular weight* (Vol. 25).

El Achkar, T., Fourmentin, S., & Greige-Gerges, H. (2019). Deep eutectic solvents: An overview on their interactions with water and biochemical compounds. *Journal of Molecular Liquids, 288*, Article 111028. https://doi.org/10.1016/j.molliq.2019.111028

Elizondo, O. M., Hiemstra, I. S. A., Chorhirankul, N., Eppink, M., Wijffels, H., Janssen, A. E. M., & Kazbar, A. (2024). Pressure-driven membrane processes for the recovery and recycling of deep eutectic solvents : A seaweed biorefinery case study. *Biotechnology Reports, 43*, Article e00849. https://doi.org/10.1016/j.btre.2024.e00849. June.

Farrés, I. F., & Norton, I. T. (2014). Formation kinetics and rheology of alginate fluid gels produced by in-situ calcium release. *Food Hydrocolloids, 40*, 76–84. https://doi.org/10.1016/j.foodhyd.2014.02.005

Fernando, I. P. S., Kim, D., Nah, J. W., & Jeon, Y. J. (2019). Advances in functionalizing fucoidans and alginates (bio)polymers by structural modifications: A review. *Chemical Engineering Journal, 355*, 33–48. https://doi.org/10.1016/j.cej.2018.08.115

Fu, S., Thacker, A., Sperger, D. M., Boni, R. L., Buckner, I. S., Velankar, S., Munson, E. J., & Block, L. H. (2011). Relevance of rheological properties of sodium alginate in solution to calcium alginate gel properties. *AAPS PharmSciTech, 12*(2), 453–460. https://doi.org/10.1208/s12249-011-9587-0

Gisbert, M., Sineiro, J., & Moreira, R. (2022). Influence of oxidation and dialysis of phlorotannins on bioactivity and composition of ultrasound-assisted extracts from Ascophyllum nodosum. *Marine Drugs, 20*(11). https://doi.org/10.3390/md20110706

Gomez, C. G., Pérez Lambrecht, M. V., Lozano, J. E., Rinaudo, M., & Villar, M. A. (2009). Influence of the extraction-purification conditions on final properties of alginates obtained from brown algae (macrocystis pyrifera). *International Journal of Biological Macromolecules, 44*(4), 365–371. https://doi.org/10.1016/j.ijbiomac.2009.02.005

Gómez-Ordóñez, E., Jiménez-Escrig, A., & Rupérez, P. (2012). Molecular weight distribution of polysaccharides from edible seaweeds by high-performance size-exclusion chromatography (HPSEC). *Talanta, 93*, 153–159. https://doi.org/10.1016/j.talanta.2012.01.067

González-gonzález, L. M., Astals, S., Pratt, S., Jensen, P. D., & Schenk, P. M. (2019). Impact of osmotic shock pre-treatment on microalgae lipid extraction and subsequent methane production. *Bioresource Technology Reports, 7*, Article 100214. https://doi.org/10.1016/j.biteb.2019.100214. April.

Halim, R., Papachristou, I., Kubisch, C., Nazarova, N., Wüstner, R., Steinbach, D., Chen, G. Q., Deng, H., Frey, W., Posten, C., & Silve, A. (2021). Hypotonic osmotic shock treatment to enhance lipid and protein recoveries from concentrated saltwater nannochloropsis slurries. *Fuel, 287*, Article 119442. https://doi.org/10.1016/j.fuel.2020.119442. November 2020.

Haug, A., & Smidsrød, O. (1962). Determination of intrinsic viscosity of alginate. *Acta Chemica Scandinavica, 7*(16).

Hermansson, E., Schuster, E., Lindgren, L., Altskär, A., & Ström, A. (2016). Impact of solvent quality on the network strength and structure of alginate gels. *Carbohydrate Polymers, 144*, 289–296. https://doi.org/10.1016/j.carbpol.2016.02.069

Hiemstra, I. S. A., Meinema, J. T., Eppink, M. M. H., & Kazbar, A. (2024). Choline chloride-based solvents as alternative media for alginate extraction from brown seaweed, 214(November) https://doi.org/10.1016/j.lwt.2024.117174.

Holme, H. K., Davidsen, L., Kristiansen, A., & Smidsrød, O. (2008). Kinetics and mechanisms of depolymerization of alginate and chitosan in aqueous solution. *Carbohydrate Polymers, 73*(4), 656–664. https://doi.org/10.1016/j.carbpol.2008.01.007

Holme, H. K., Lindmo, K., Kristiansen, A., & Smidsrød, O. (2003). *Thermal depolymerization of alginate in the solid state*. https://doi.org/10.1016/S0144-8617(03)00134-6

House, K. A., & House, J. E. (2017). Thermodynamics of dissolution of urea in water , alcohols , and their mixtures. *Journal of Molecular Liquids, 242*, 428–432. https://doi.org/10.1016/j.molliq.2017.07.020.

Huang, Z., Wu, B., Wen, Q., Yang, T., & Yang, Z. (2014). Deep eutectic solvents can be viable enzyme activators and stabilizers. December 2013 https://doi.org/10.1002/jctb.4285.

Hurtado, A., Aljabali, A. A. A., Mishra, V., Tambuwala, M. M., & Serrano-Aroca, Á. (2022). Alginate: Enhancement strategies for advanced applications. *International Journal of Molecular Sciences, 23*(9). https://doi.org/10.3390/ijms23094486

Jiang, L., & Zheng, K. (2023). Electronic structures of zwitterionic and protonated forms of glycine betaine in water: Insights into solvent effects from ab initio simulations. *Journal of Molecular Liquids, 369*. https://doi.org/10.1016/j.molliq.2022.120871

Jørgensen, T. E., Sletmoen, M., Draget, K. I., & Stokke, B. T. (2007). Influence of oligoguluronates on alginate gelation. *Kinetics , and polymer organization*.

Kasaai, M. R. (2006). Intrinsic viscosity-molecular weight relationship and hydrodynamic volume for pullulan. *Journal of Applied Polymer Science, 100*(6), 4325–4332. https://doi.org/10.1002/app.22324

Kholany, M., Reynaga-Navarro, W., Abranches, D. O., Wijffels, R., Coutinho, J. A. P., Ventura, S. P. M., & Kazbar, A. (2025). Extraction and separation of pigments from Saccharina latissima using eutectic solvents. *Separation and Purification Technology, 357*, Article 130053. https://doi.org/10.1016/j.seppur.2024.130053

Kholany, M., Schaeffer, N., Macário, I. P. E., Veloso, T., Caetano, T., Pereira, J. L., Schaeffer, N., Dias, A. C. R. V., Coutinho, J. A. P., & Ventura, S. P. M. (2023). Unveiling the use of hydrophobic eutectic solutions as Task- specific solvents to recover bacterioruberin from Haloferax mediterranei. *Sustainable Chemistry & Engineering*. https://doi.org/10.1021/acssuschemeng.3c02997

Kwon, Y. J., Kwon, O. I., Hwang, H. J., Shin, H. C., & Yang, S. (2023). Therapeutic effects of phlorotannins in the treatment of neurodegenerative disorders. In *Frontiers in molecular neuroscience* (Vol. 16). Frontiers Media S.A. https://doi.org/10.3389/fnmol.2023.1193590

Larsen, B. E., Bjørnstad, J., Pettersen, E. O., Tønnesen, H. H., & Melvik, J. E. (2015). Rheological characterization of an injectable alginate gel system. *BMC Biotechnology, 15*(1). https://doi.org/10.1186/s12896-015-0147-7

Lever, M., & Slow, S. (2010). The clinical significance of betaine, an osmolyte with a key role in methyl group metabolism. *Clinical Biochemistry, 43*(9), 732–744. https://doi.org/10.1016/j.clinbiochem.2010.03.009

Li, D. (2022). Natural deep eutectic solvents in phytonutrient extraction and other applications. *Frontiers in Plant Science, 13*, Article 1004332. https://doi.org/10.3389/fpls.2022.1004332.

Li, P., Yang, C., Jiang, Z., Jin, Y., & Wu, W. (2023). Lignocellulose pretreatment by deep eutectic solvents and related technologies: A review. *Journal of Bioresources and Bioproducts, 8*(1), 33–44. https://doi.org/10.1016/j.jobab.2022.11.004

Lim, S. J., Mustapha, W., & Aida, W. (2017). Extraction of sulfated polysaccharides (fucoidan) from brown seaweed. In *Seaweed polysaccharides*. Elsevier Inc. https://doi.org/10.1016/B978-0-12-809816-5/00003-7.

Liu, Y., Friesen, J. B., McAlpine, J. B., Lankin, D. C., Chen, S. N., & Pauli, G. F. (2018). Natural deep eutectic solvents: Properties, applications, and perspectives. In *Journal of natural products* (Vol. 81, pp. 679–690). American Chemical Society. https://doi.org/10.1021/acs.jnatprod.7b00945

Lomartire, S., & Gonçalves, A. M. M. (2022). Novel technologies for seaweed polysaccharides extraction and their use in food with therapeutically applications—A review. *Foods, 11*(17). https://doi.org/10.3390/foods11172654

Loow, Y. L., New, E. K., Yang, G. H., Ang, L. Y., Foo, L. Y. W., & Wu, T. Y. (2017). Potential use of deep eutectic solvents to facilitate lignocellulosic biomass utilization and conversion. *Cellulose, 24*(9), 3591–3618. https://doi.org/10.1007/s10570-017-1358-y

Ma, J., Lin, Y., Chen, X., Zhao, B., & Zhang, J. (2014). Flow behavior, thixotropy and dynamical viscoelasticity of sodium alginate aqueous solutions. *Food Hydrocolloids, 38*, 119–128. https://doi.org/10.1016/j.foodhyd.2013.11.016

Matchim Kamdem, M. C., Tamafo Fouegue, A. D., & Lai, N. (2023). A comprehensive study on DES pretreatment application to microalgae for enhanced lipid recovery suitable for biodiesel production: Combined experimental and theoretical investigations. *Energies, 16*(9). https://doi.org/10.3390/en16093806

Montes, L., Gisbert, M., Hinojosa, I., & Sineiro, J. (2021). Impact of drying on the sodium alginate obtained after polyphenols ultrasound-assisted extraction from Ascophyllum nodosum seaweeds, 272(July) https://doi.org/10.1016/j.carbpol.2021.118455.

Moradiya, K., & Pereira, M. M. (2024). *Aqueous solution of ionic liquid is an efficient substituting solvent system for the extraction of alginate from Sargassum tenerrimum* (pp. 116–129).

Moreira, A. S. P., Gaspar, D., Ferreira, S. S., Correia, A., Vilanova, M., Perrineau, M. M., Kerrison, P. D., Gachon, C. M. M., Domingues, M. R., Coimbra, M. A., Coreta-Gomes, F. M., & Nunes, C. (2023). Water-soluble Saccharina latissima polysaccharides and relation of their structural characteristics with in vitro immunostimulatory and hypocholesterolemic activities. *Marine Drugs, 21*(3). https://doi.org/10.3390/md21030183

Naik, P. K., Kumar, N., Paul, N., & Banerjee, T. (2022). Deep eutectic solvents in liquid–liquid extraction. In *Deep eutectic solvents in liquid–liquid extraction*. https://doi.org/10.1201/9781003231158

Natalello, A., Liu, J., Ami, D., Doglia, S. M., & De Marco, A. (2009). The osmolyte betaine promotes protein misfolding and disruption of protein aggregates. *Proteins: Structure, Function, and Bioinformatics, 75*(2), 509–517. https://doi.org/10.1002/prot.22266

Nava-Ocampo, M. F., Al Fuhaid, L., Santana, A., Bucs, S. S., Verpoorte, R., Hae Choi, Y., Witkamp, G. J., Vrouwenvelder, J. S., & Farinha, A. S. F. (2021). Structural properties and stability of the betaine-urea natural deep eutectic solvent. *Journal of Molecular Liquids, 343*. https://doi.org/10.1016/j.molliq.2021.117655

Neoh, Y. Y., Matanjun, P., & Lee, J. S. (2016). Comparative study of drying methods on chemical constituents of Malaysian red seaweed. *Drying Technology, 34*(14), 1745–1751. https://doi.org/10.1080/07373937.2016.1212207

Neves, M. I., Moroni, L., & Barrias, C. C. (2020). Modulating alginate hydrogels for improved biological performance as cellular 3D microenvironments. *Frontiers in Bioengineering and Biotechnology, 8*(June). https://doi.org/10.3389/fbioe.2020.00665

Norton, I. T., Spyropoulos, F., & Cox, P. (2011). *Practical food rheology : An interpretive approach*. Blackwell.

Olivares, B., Martínez, F. A., Ezquer, M., Morales, B. J., Fuentes, I., Calvo, M., & Campodónico, P. R. (2022). Betaine-urea deep eutectic solvent improves imipenem antibiotic activity. *Journal of Molecular Liquids, 350*. https://doi.org/10.1016/j.molliq.2022.118551.

Patel, A. D., & Desai, M. A. (2023). Progress in the field of hydrotropy: Mechanism, applications and green concepts. *Reviews in Chemical Engineering, 39*(4), 601–630. https://doi.org/10.1515/revce-2021-0012

Postma, P. R., Cerezo-Chinarro, O., Akkerman, R. J., Olivieri, G., Wijffels, R. H., Brandenburg, W. A., & Eppink, M. H. M. (2018). Biorefinery of the macroalgae ulva

lactuca: Extraction of proteins and carbohydrates by mild disintegration. *Journal of Applied Phycology, 30*(2), 1281–1293. https://doi.org/10.1007/s10811-017-1319-8
Qosim, N., Dai, Y., Williams, G. R., & Edirisinghe, M. (2024). Structure, properties, forming, and applications of alginate fibers: A review. *International Materials Reviews, 69*(5–6), 309–333. https://doi.org/10.1177/09506608241280419
Rahman, M. M., Shahid, M. A., Hossain, M. T., Sheikh, M. S., Rahman, M. S., Uddin, N., Rahim, A., Khan, R. A., & Hossain, I. (2024). Sources, extractions, and applications of alginate: A review. In *Discover applied sciences* (Vol. 6). Springer Nature. https://doi.org/10.1007/s42452-024-06151-2. Issue 8.
Ressl, S., Terwisscha Van Scheltinga, A. C., Vonrhein, C., Ott, V., & Ziegler, C. (2009). Molecular basis of transport and regulation in the na+/Betaine symporter BetP. *Nature, 458*(7234), 47–52. https://doi.org/10.1038/nature07819
Reynaga-Navarro, W., Wijffels, R. H., & michel. (2024). Isolation and quantification of alginate in choline chloride-based deep eutectic solvents. *International Journal of Biological Macromolecules, 262*. https://doi.org/10.1016/j.ijbiomac.2024.130103. January.
Rinaudo, M. (2007). Seaweed polysaccharides. In H. Kamerling (Ed.), *Comprehensive glycoscience* (pp. 691–735). Elsevier Ltd. https://doi.org/10.1016/B978-044451967-2/00140-9.
Rockinger, U., Funk, M., & Winter, G. (2021). Current approaches of preservation of cells during (freeze-) drying. In *Journal of pharmaceutical sciences, 110* pp. 2873–2893). Elsevier B.V. https://doi.org/10.1016/j.xphs.2021.04.018
Roopa, B. S., & Bhattacharya, S. (2008). Alginate gels: I. Characterization of textural attributes. *Journal of Food Engineering, 85*(1), 123–131. https://doi.org/10.1016/j.jfoodeng.2007.07.012
Rupérez, P., Ahrazem, O., & Leal, J. A. (2002). Potential antioxidant capacity of sulfated polysaccharides from the edible marine brown seaweed fucus vesiculosus. *Journal of Agricultural and Food Chemistry, 50*(4), 840–845. https://doi.org/10.1021/jf010908o
Sahoo, D. R., & Biswal, T. (2021). Alginate and its application to tissue engineering. In *SN applied sciences* (Vol. 3). Springer Nature. https://doi.org/10.1007/s42452-020-04096-w
Saji, S., Hebden, A., Goswami, P., & Du, C. (2022). A brief review on the development of alginate extraction process and its sustainability. *Sustainability, 14*(9), 5181. https://doi.org/10.3390/su14095181
Saravana, P. S., Cho, Y. N., Woo, H. C., & Chun, B. S. (2018). Green and efficient extraction of polysaccharides from brown seaweed by adding deep eutectic solvent in subcritical water hydrolysis. *Journal of Cleaner Production, 198*, 1474–1484. https://doi.org/10.1016/j.jclepro.2018.07.151
Saravana, P. S., Ho, T. C., Chae, S. J., Cho, Y. J., Park, J. S., Lee, H. J., & Chun, B. S. (2018). Deep eutectic solvent-based extraction and fabrication of chitin films from crustacean waste. *Carbohydrate Polymers, 195*(March), 622–630. https://doi.org/10.1016/j.carbpol.2018.05.018
Sardari, R. R. R., Prothmann, J., Gregersen, O., & Turner, C. (2021). Identification of phlorotannins in the brown algae , Saccharina latissima and Ascophyllum nodosum by ultra-high-performance liquid chromatography coupled to high-resolution tandem mass spectrometry. *Molecules, 26*.
Shao, Z., & Duan, D. (2022). The cell wall polysaccharides biosynthesis in seaweeds : A molecular perspective, 13(May), 1–7 https://doi.org/10.3389/fpls.2022.902823.
Shrivastava, A. (2018). Polymerization. In *Introduction to plastics engineering* (pp. 17–48). Elsevier. https://doi.org/10.1016/B978-0-323-39500-7.00002-2.
Silva, A. F. R., Abreu, H., Silva, A. M. S., & Cardoso, S. M. (2019). Effect of oven-drying on the recovery of valuable compounds from Ulva rigida, gracilaria sp. and fucus vesiculosus. *Marine Drugs, 17*(2). https://doi.org/10.3390/md17020090
Stern, J. L., Hagerman, A. E., Steinberg, P. D., & Mason, P. K. (1996). Phlorotannin-protein interactions. *Journal of Chemical Ecology, 22*(10), 1877–1899. https://doi.org/10.1007/BF02028510
Storz, H., Müller, K. J., Ehrhart, F., Gómez, I., Shirley, S. G., Gessner, P., Zimmermann, G., Weyand, E., Sukhorukov, V. L., Forst, T., Weber, M. M., Zimmermann, H., Kulicke, W. M., & Zimmermann, U. (2009). Physicochemical features of ultra-high viscosity alginates. *Carbohydrate Research, 344*(8), 985–995. https://doi.org/10.1016/j.carres.2009.02.016
Sweeney, T., & O'Doherty, J. V. (2016). Marine macroalgal extracts to maintain gut homeostasis in the weaning piglet. In *Domestic animal endocrinology* (Vol. 56, pp. S84–S89). Elsevier Inc. https://doi.org/10.1016/j.domaniend.2016.02.002
Turck, D., Castenmiller, J., Henauw, S. De, Hirsch-ernst, K. I., Kearney, J., Maciuk, A., Mangelsdorf, I., Mcardle, H. J., Naska, A., Pelaez, C., Pentieva, K., Siani, A., Thies, F., Tsabouri, S., Vinceti, M., Cubadda, F., Engel, K. H., Frenzel, T., Heinonen, M., Marchelli, R., Annette, P., Poulsen, M., Sanz, Y., & Neuh, M. (2019). *Safety of Betaine as a Novel Food Pursuant to Regulation (EU) 2015/2283. 17(March)*. https://doi.org/10.2903/j.efsa.2019.5658.
U.S. Food and Drug Administration. (2025). *Title 21, § 184.1923. In Electronic Code of Federal Regulations*. Retrieved July 9, 2025, from https://www.ecfr.gov/current/title-21/chapter-I/subchapter-B/part-184/subpart-B/section-184.1923.
Veide Vilg, J., & Undeland, I. (2017). pH-driven solubilization and isoelectric precipitation of proteins from the brown seaweed saccharina Latissima—Effects of osmotic shock, water volume and temperature. *Journal of Applied Phycology, 29*(1), 585–593. https://doi.org/10.1007/s10811-016-0957-6
Wang, J., Teng, C., & Yan, L. (2022). Applications of deep eutectic solvents in the extraction, dissolution, and functional materials of chitin: Research progress and prospects, 552–564 https://doi.org/10.1039/d1gc04340d.
Wang, S., Qin, L., Zhou, Z., & Wang, J. (2012). *Solubility and Solution Thermodynamics of Betaine in Different Pure Solvents and Binary Mixtures*. https://doi.org/10.1021/je2011659
Xu, H., Peng, J., Kong, Y., Liu, Y., Su, Z., Li, B., Song, X., Liu, S., & Tian, W. (2020). Key process parameters for deep eutectic solvents pretreatment of lignocellulosic biomass materials: A review. In *Bioresource technology, 310*. Elsevier Ltd. https://doi.org/10.1016/j.biortech.2020.123416
Yang, J., Chen, S., & Fang, Y. (2009). Viscosity study of interactions between sodium alginate and CTAB in dilute solutions at different pH values. *Carbohydrate Polymers, 75*(2), 333–337. https://doi.org/10.1016/j.carbpol.2008.07.037
Yang, J., Sui, X., Li, Q., Zhao, W., & Zhang, J. (2019a). In Situ encapsulation of postcryopreserved cells using alginate polymer and zwitterionic betaine. https://doi.org/10.1021/acsbiomaterials.9b00249.
Yang, J., Sui, X., Li, Q., Zhao, W., & Zhang, J. (2019b). In Situ encapsulation of postcryopreserved cells using alginate polymer and zwitterionic betaine. https://doi.org/10.1021/acsbiomaterials.9b00249.
Yang, T. X., Zhao, L. Q., Wang, J., Song, G. L., Liu, H. M., Cheng, H., & Yang, Z. (2017). Improving whole-cell biocatalysis by addition of deep eutectic solvents and natural deep eutectic solvents. *ACS Sustainable Chemistry & Engineering, 5*(7), 5713–5722. https://doi.org/10.1021/acssuschemeng.7b00285
Yong, K., & Mooney, D. J. (2012). Alginate: Properties and biomedical applications. *Progress in Polymer Science, 37*(1), 106–126. https://doi.org/10.1016/j.progpolymsci.2011.06.003
Zayed, A., El-aasr, M., Ibrahim, A. S., & Ulber, R. (2020). *Fucoidan characterization : Determination of purity and physicochemical and chemical properties* (Vols. 1–31). https://doi.org/10.3390/md18110571
Zeng, C. X., Qi, S. J., Xin, R. P., Yang, B., & Wang, Y. H. (2016). Synergistic behavior of betaine-urea mixture: Formation of deep eutectic solvent. *Journal of Molecular Liquids, 219*, 74–78. https://doi.org/10.1016/j.molliq.2016.02.076
Zhang, S., Dong, J., Pan, R., Xu, Z., Li, M., & Zang, R. (2023). Structures, properties, and bioengineering applications of alginates and hyaluronic acid. *Polymers, 15*(9). https://doi.org/10.3390/polym15092149
Zheng, M., Hong, J., Chuai, P., Chen, Y., Ni, H., Li, Q., & Jiang, Z. (2022). Impacts of agar gum and fucoidan on gel properties of surimi products without phosphate. *Food Science and Nutrition, 10*(11), 3759–3771. https://doi.org/10.1002/fsn3.2973
Zhu, B., & Yin, H. (2015). *Alginate lyase: Review of major sources and classification, properties, structure-function analysis and applications. June* (pp. 125–131). https://doi.org/10.1080/21655979.2015.1030543.